

# We are IntechOpen, the world's leading publisher of Open Access books Built by scientists, for scientists

6,900

Open access books available

186,000

International authors and editors

200M

Downloads

Our authors are among the

154

Countries delivered to

TOP 1%

most cited scientists

12.2%

Contributors from top 500 universities



WEB OF SCIENCE™

Selection of our books indexed in the Book Citation Index  
in Web of Science™ Core Collection (BKCI)

Interested in publishing with us?  
Contact [book.department@intechopen.com](mailto:book.department@intechopen.com)

Numbers displayed above are based on latest data collected.  
For more information visit [www.intechopen.com](http://www.intechopen.com)



---

# Complex Systems with Self-Elimination of Dissipation with Implication in Bio-Structural Behavior Via Nondifferentiability

---

Maricel Agop, Decebal Vasincu, Daniel Timofte, Elena Simona Bacaita, Andrei Agop and Stefan Andrei Irimiciuc

Additional information is available at the end of the chapter

<http://dx.doi.org/10.5772/67939>

---

## Abstract

In the present chapter, we show that the use of the nondifferentiable mathematical procedures, developed in the Scale Relativity Theory with constant arbitrary fractal dimension, simplifies very much the dynamics analyses in the case of complex systems. By applying such a procedure to various complex systems dynamics (biological structures, ablation or discharge plasmas, etc.), we are able to observe that it starts from a steady (oscillating state) and as the external factor is varied the system undergoes significant changes. The systems evolve asymptotically through various transition, toward a chaotic regime (like bifurcations or intermittencies), but never reaching it. Another important reveal from the study of the system's dynamics was the presence of various steady states depending on the resolution scale at which the theoretical investigations are performed.

**Keywords:** complex systems, fractal model, chaos, biological systems

---

## 1. Introduction

Complex systems, encountered in human societies, neural networks, the Internet, ecosystems, biological evolution, stock markets, economies, and many others, represent interdisciplinary research topics that have been studied by means of some fundamental theories, especially from physics and computer simulation. These systems are composed of a high number of individual components and their evolution cannot be predicted simply by analyzing the individual behavior of their elements or by adding their behavior. Their global evolution is decisively influenced by the manner in which the elements relate to each other,

---

leading to emergence, self-organization, and adaptability [1–3]. Correspondingly, the theoretical models corresponding to the complex systems dynamics become sophisticated [2, 3].

The models can be strongly simplified by taking into account that the complexity of interaction process imposes various temporal resolution scales, and the pattern evolution imposes different degrees of freedom [4]. Thus, new theoretical models can be developed by admitting that the complex systems that display chaotic behavior are recognized to acquire self-similarity in association with strong fluctuations at all possible space-time scales [5, 6]. Then, for large temporal scales compared to the inverse of the highest Lyapunov exponent [7–10], instead of deterministic trajectories we will work with a collection of potential trajectories and instead of definite positions with probability density. One interesting example is the case of collisions in complex system, where the dynamics of the particles can be described by nondifferentiable curves.

Therefore, in order to build a theoretical model for the evolution of complex systems, the fundamentals of a nondifferentiable physics must be defined. For this, the system complexity is substituted with the nondifferentiable character of physical quantities, idea that lies at the base of Scale Relativity Theory (SRT) [11, 12] and of the nonstandard Scale Relativity Theory (NSRT), a particular case of the first one for a fractal dimension arbitrary constant [13]. In the framework of the above two theories, assuming that the individual components of the complex system move on continuous, but nondifferentiable curves, named fractal curves, the evolution of complex systems can be described by physical quantities depending both on the well-known space-time coordinates and, besides that, on the space-time scales resolution; thus, it can be considered fractal functions [11, 13]. Moreover, the complex system will act as a “fluid” without interactions because its individual components are reduced to and identified with their own trajectories, named geodesics.

Further, we show that the dynamics “control” of various complex systems (biological structures, ablation, discharge plasmas, etc.) can be realized by means of fractality.

## 2. Complex systems: mathematical model

Taking into consideration the above, the following consequences emerge regarding the complex systems dynamics [11–13]:

- i. any trajectory of the individual components (fractal fluid line) is explicitly dependent on scale resolution  $\delta t$ ;
- ii. applying the substitution principle,  $\delta t \equiv dt$ , the scale resolution can be considered as an independent variable. We reserve the notation  $dt$  for the usual time as in the Hamiltonian complex system dynamics;
- iii. the variables that appear in the dynamics of complex system are fractal, i.e., are functions that depends both on the space-time coordinates and on the scale resolution. Then, in any point of the fractal curve, two derivatives of the variable field  $M(t, dt)$  as explicit functions of the two variables  $t$  and  $dt$ , can be defined:

$$\begin{aligned} \frac{d_+M(t, dt)}{dt} &= \lim_{\Delta t \rightarrow 0_+} \frac{M(t + \Delta t, \Delta t) - M(t, \Delta t)}{\Delta t} \\ \frac{d_-M(t, dt)}{dt} &= \lim_{\Delta t \rightarrow 0_-} \frac{M(t, \Delta t) - M(t - \Delta t, \Delta t)}{\Delta t} \end{aligned} \quad (1)$$

The “+” sign indicates forward processes and the “-” sign to the backwards ones;

- iv. the differential of the spatial coordinate field  $dX^i(t, dt)$  is expressed as:

$$d_{\pm}X^i(t, dt) = d_{\pm}x^i(t) + d_{\pm}\xi^i(t, dt) \quad (2)$$

where  $d_{\pm}x^i(t)$  is the “classical part” (differentiable, scale resolution independent) and  $d_{\pm}\xi^i(t, dt)$  is the “fractal part” (nondifferentiable, scale resolution dependent);

- v. the nondifferentiable part of the spatial coordinate field, by means of which we can describe the complex system dynamics, satisfies the fractal equation [5]:

$$d_{\pm}\xi^i = \lambda_{\pm}^i(dt)^{1/D_F} \quad (3)$$

where  $\lambda_{\pm}^i$  are constant coefficients through which the fractalization type describing the complex system dynamics is specified and  $D_F$  defines the fractal dimension of the motion non-differentiable curve.

In our opinion, the complex system processes imply a dynamics on geodesics with various fractal dimensions. The variety of these fractal dimensions of the complex system geodesics comes as a result of complex system structure. Precisely, for  $D_F = 2$ , quantum type processes are generated in the complex system, for  $D_F < 2$  correlative type processes are induced and for  $D_F > 2$  noncorrelative type ones can be found (for details, see [8, 14]);

- vi. the differential time reflection invariance of any dynamical variable of the complex system is recovered by combining the derivatives  $d_+/dt$  and  $d_-/dt$  in the nondifferentiable operator

$$\frac{\hat{\partial}}{\partial t} = \frac{1}{2} \left( \frac{d_+ + d_-}{dt} \right) - \frac{i}{2} \left( \frac{d_+ - d_-}{dt} \right) \quad (4)$$

This is a natural result of the complex prolongation procedure applied to complex system dynamics [13, 15]. Applying now the nondifferentiable operator to the spatial coordinate field, by means of which we can describe the fractal fluid dynamics, yields the complex velocity field of the fractal fluid:

$$\hat{V}^i = \frac{\hat{d}X^i}{dt} = \mathbf{V}_D^i - V_F^i \quad (5)$$

with:

$$\begin{aligned} V_D^i &= \frac{1}{2} \left( \frac{d_+ X^i + d_- X^i}{dt} \right) \\ V_F^i &= \frac{1}{2} \left( \frac{d_+ X^i - d_- X^i}{dt} \right) \end{aligned} \quad (6)$$

The real part,  $V_D^i$ , represents the “classical velocity” (differentiable, i.e., scale resolution independent), while the imaginary part,  $V_F^i$ , is the “fractal velocity” (nondifferentiable, i.e., scale resolution dependent), induced by fractality;

- vii. any external constraint is equivalent with a selection of fractal fluid geodesics, whose nondifferentiability, together with the two values of the derivative imply a generalized statistical fluid-like description. Then, the average of  $d_{\pm} X^i$  is:

$$\langle d_{\pm} X^i \rangle = d_{\pm} x^i \quad (7)$$

with

$$\langle d_{\pm} \xi^i \rangle = 0 \quad (8)$$

The previous relation (8) means that the average of the fractal fluctuations is null;

- viii. in order to determine the scale covariant derivative, which describes the fractal fluid dynamics, we will consider that the individual components of the complex fluid move in a three-dimensional space and that  $X^i$  are the spatial coordinates of a point on their nondifferentiable curves. The second-order Taylor expansion for a variable field  $M(X^i, t)$  is:

$$d_{\pm} M(X^i, t) = \partial_t M dt + \partial_i M \cdot d_{\pm} X^i + \frac{1}{2} \partial_i \partial_k M \cdot d_{\pm} X^i d_{\pm} X^k \quad (9)$$

These relations are valid in any point and more for the points  $X^i$  on the nondifferentiable curve which we have selected in Eq. (9). From here, forward and backward values for fractal fluid variables from Eq. (9) become:

$$\langle d_{\pm} M \rangle = \langle \partial_t M dt \rangle + \langle \partial_i M \cdot d_{\pm} X^i \rangle + \frac{1}{2} \langle \partial_i \partial_k M \cdot d_{\pm} X^i d_{\pm} X^k \rangle \quad (10)$$

Assuming that the differentials  $d_{\pm} X^i$ ,  $dt$  are independent and the mediated values of all variables and their derivatives coincide with themselves, relation (10) becomes:

$$d_{\pm} M = \partial_t M dt + \partial_i M \cdot \langle d_{\pm} X^i \rangle + \frac{1}{2} \partial_i \partial_k M \cdot \langle d_{\pm} X^i d_{\pm} X^k \rangle \quad (11)$$

Using Eq. (3), for  $i \neq j$  we can write:

$$\langle d_{\pm} \xi^l d_{\pm} \xi^k \rangle = \pm \lambda_{\pm}^l \lambda_{\pm}^k (dt)^{(2/D_F)-1} dt \quad (12)$$

where the signs “+” and “-” have the same significance as in relation (1).

Then, Eq. (11) takes the form:

$$d_{\pm} M = \partial_t M dt + \partial_i M \cdot \langle d_{\pm} X^i \rangle + \frac{1}{2} \partial_i \partial_k M \cdot d_{\pm} x^l d_{\pm} x^k + \frac{1}{2} \partial_i \partial_k M [\lambda_{\pm}^l \lambda_{\pm}^k (dt)^{(2/D_F)-1} dt] \quad (13)$$

Using the method from [11–13], which involves dividing by  $dt$  and neglecting the terms with differential factors, we obtain:

$$\frac{d_{\pm} M}{dt} = \partial_t M + v_{\pm}^i \cdot \partial_i M + \frac{1}{2} \lambda_{\pm}^l \lambda_{\pm}^k (dt)^{(2/D_F)-1} \partial_i \partial_k M \quad (14)$$

with

$$v_{\pm}^i = \frac{d_{\pm} x^i}{dt}$$

These relations also allow us to define the operator:

$$\frac{d_{\pm}}{dt} = \partial_t + v_{\pm}^i \cdot \partial_i + \frac{1}{2} \lambda_{\pm}^l \lambda_{\pm}^k (dt)^{(2/D_F)-1} \partial_i \partial_k \quad (15)$$

Considering Eqs. (4), (5), and (15), it results:

$$\frac{\hat{d}M}{dt} = \partial_t M + \hat{V}^i \cdot \partial_i M + \frac{1}{4} (dt)^{(2/D_F)-1} D^{lk} \partial_l \partial_k M \quad (16)$$

where

$$\begin{aligned} D^{lk} &= d^{lk} - i \bar{d}^{lk} \\ d^{lk} &= \lambda_{+}^l \lambda_{+}^k - \lambda_{-}^l \lambda_{-}^k, \bar{d}^{lk} = \lambda_{+}^l \lambda_{+}^k + \lambda_{-}^l \lambda_{-}^k \end{aligned} \quad (17)$$

Using Eq. (16), the scale covariant derivative in the fractal fluid dynamics is defined as:

$$\frac{\hat{d}}{dt} = \partial_t + \hat{V}^i \cdot \partial_i + \frac{1}{4} (dt)^{(2/D_F)-1} D^{lk} \partial_l \partial_k \quad (18)$$

### 3. Fractal fluid geodesics

Based on the scale covariance principle (physics laws are invariant in respect to all scale transformations), we will consider that the transition from classical to nondifferentiable physics is equivalent with the replacement of standard derivative  $d/dt$  with the nondifferentiable operator  $\hat{d}/dt$ . In consequence, it will act as scale covariant derivative, applied for writing the equations of fractal fluid dynamics in similar forms to those from the classical (differentiable)

physics. Thus, the operator (18) applied to the complex velocity (5), with no external constraint, implies the geodesics in the following form:

$$\frac{\hat{d}\hat{V}^i}{dt} = \partial_t \hat{V}^i + \hat{V}^l \cdot \partial_l \hat{V}^i + \frac{1}{4} (dt)^{(2/D_F)-1} D^{lk} \partial_l \partial_k \hat{V}^i = 0 \quad (19)$$

This means that the local acceleration  $\partial_t \hat{V}^i$ , the convection  $\hat{V}^l \cdot \partial_l \hat{V}^i$ , and the dissipation  $D^{lk} \partial_l \partial_k \hat{V}^i$  make their balance in any point of the nondifferentiable curve. Moreover, the presence of the complex coefficient,  $4^{-1} (dt)^{(2/D_F)-1} D^{lk}$ , indicates that the fractal fluid has rheological properties, such as memory, determined by its internal structure.

Considering that the fractalization is induced by Markov-type stochastic processes, with individual components displacements of Lévy type [16, 17], then:

$$\lambda_+^i \lambda_+^l = \lambda_-^i \lambda_-^l = 2\lambda \delta^{il} \quad (20)$$

where  $\delta^{il}$  is the Kronecker's pseudo-tensor.

In these conditions, Eq. (19) becomes:

$$\frac{\hat{d}\hat{V}^i}{dt} = \partial_t \hat{V}^i + \hat{V}^l \cdot \partial_l \hat{V}^i - i\lambda (dt)^{(2/D_F)-1} \partial^l \partial_l \hat{V}^i = 0 \quad (21)$$

Separating the individual components movements on differential and fractal scale resolutions, Eq. (21) becomes equivalent with the equations set:

$$\begin{aligned} \frac{\hat{d}V_D^i}{dt} &= \partial_t V_D^i + V_D^l \cdot \partial_l V_D^i - [V_F^l - \lambda (dt)^{(2/D_F)-1} \partial^l] \partial_l V_F^i = 0 \\ \frac{\hat{d}V_F^i}{dt} &= \partial_t V_F^i + V_D^l \cdot \partial_l V_F^i - [V_F^l - \lambda (dt)^{(2/D_F)-1} \partial^l] \partial_l V_D^i = 0 \end{aligned} \quad (22)$$

#### 4. Geodesics in the Schrödinger-type representation

For irrotational motions, the complex velocity satisfies the condition:

$$\varepsilon_{ikl} \partial^k \hat{V}^l = 0 \quad (23)$$

where  $\varepsilon_{ikl}$  is the Levi-Civita pseudo-tensor. Then, the complex velocity field becomes:

$$\hat{V}^i = -2i\lambda (dt)^{(2/D_F)-1} \partial^i \ln \Psi \quad (24)$$

where for the moment,  $\ln \Psi$  defines the scalar potential of the complex velocity field. Substituting Eq. (24) in Eq. (22), it results:

$$\frac{\hat{d}\hat{V}^i}{dt} = -2i\lambda(dt)^{(2/D_F)-1} \{ \partial_i \partial^i \ln \Psi - i[2\lambda(dt)^{(2/D_F)-1} (\partial^l \ln \Psi \partial_l) \partial^i \ln \Psi + \lambda(dt)^{(2/D_F)-1} \partial^l \partial_l \partial^i \ln \Psi] \} = 0 \quad (25)$$

or using the identities:

$$\begin{aligned} \partial^l \partial_l \ln \Psi + \partial_i \ln \Psi \partial^i \ln \Psi &= \frac{\partial_l \partial^l \Psi}{\Psi} \\ \partial^i \left( \frac{\partial_l \partial^l \Psi}{\Psi} \right) &= 2(\partial^l \ln \Psi \partial_l) \partial^i \ln \Psi + \partial^l \partial_l \partial^i \ln \Psi \end{aligned} \quad (26)$$

the equation:

$$\frac{\hat{d}\hat{V}^i}{dt} = -2i\lambda(dt)^{(2/D_F)-1} \partial^i \left[ \partial_t \ln \Psi - 2i\lambda(dt)^{(2/D_F)-1} \frac{\partial^l \partial_l \ln \Psi}{\Psi} \right] = 0 \quad (27)$$

By integration up to an arbitrary factor, set to zero by a suitable choice of  $\Psi$  phase, from Eq. (27) it results:

$$\lambda^2(dt)^{(4/D_F)-2} \partial^l \partial_l \Psi + i\lambda(dt)^{(2/D_F)-1} \partial_t \Psi = 0 \quad (28)$$

This is an equation of Schrödinger type, describing geodesics in the Schrödinger representation. It is reduced to the usual Schrödinger equation for motions on Peano-type curves,  $D_F = 2$  [12–14], at Compton scale,  $\lambda = \hbar/2m_0$ , where  $\hbar$  is the reduced Planck's constant and  $m_0$  the rest mass of the particle. In the presence of an external constrain, defined by a scalar potential  $U$ , Eq. (28) can be written in the form:

$$\lambda^2(dt)^{(4/D_F)-2} \partial^l \partial_l \Psi + i\lambda(dt)^{(2/D_F)-1} \partial_t \Psi - \frac{U}{2} \Psi = 0 \quad (29)$$

The relation (29) corresponds to the equation of motion for the “one body problem” in the Schrödinger-type representation of the nondifferentiable model.

The standard equation of motion for the “one body problem” in the Scale Relativity Theory [12–14]:

$$D^2 \partial^l \partial_l \Psi + iD \partial_t \Psi - \frac{U}{2} \Psi = 0 \quad (30)$$

results from Eq. (29) for movements of the complex system particles on Peano-type curves, i.e.,  $D_F = 2$  and the correspondence  $\lambda \equiv D$ , where  $D$  is the coefficient of the fractal-nonfractal transition from Scale Relativity Theory [12–14].

From such a view, in order to obtain the equations of motion for the “two-body problem” in the Schrödinger-type representation of the nondifferentiable model, we will apply a procedure which involves the next steps:

- i. the equations of motion for the “two-body problem” are written in the complex momentum representation:

$$\frac{\hat{d}P_1^l}{dt} = \partial_1^l \Phi, \quad \frac{\hat{d}P_2^l}{dt} = -\partial_2^l \Phi \quad (31)$$

where

$$P_1^l = m_1 \hat{V}_1^l, \quad P_2^l = m_2 \hat{V}_2^l \quad (32)$$

are the complex momenta,  $\hat{V}_1^l$  and  $\hat{V}_2^l$  are the complex velocities,  $m_1$  and  $m_2$  are the rest masses of the “bodies” and  $\Phi$  is the scalar potential of the interaction forces.

- ii. let’s consider that the motions are irrotational, i.e.,

$$\hat{V}_1^l = -2i\lambda_1(dt)^{(2/D_F)-1} \partial_1^l \ln \Psi_1, \quad \hat{V}_2^l = -2i\lambda_2(dt)^{(2/D_F)-1} \partial_2^l \ln \Psi_2 \quad (33)$$

where  $\ln \Psi_1$  and  $\ln \Psi_2$  are the scalar potentials of the complex velocities associated to the physical objects.

- iii. substituting Eq. (33) in Eq. (31) and following the method described above, the equations of motions of the “bodies” in the absence of direct contact are obtained in the form:

$$\begin{aligned} 2m_1\lambda_1(dt)^{(2/D_F)-1} \partial_t \Psi_1 &= [-2m_1\lambda_1^2(dt)^{(4/D_F)-2} \partial^{1l} \partial_{1l} + \Phi] \Psi_1 \\ 2m_2\lambda_2(dt)^{(2/D_F)-1} \partial_t \Psi_2 &= [-2m_2\lambda_2^2(dt)^{(4/D_F)-2} \partial^{2l} \partial_{2l} - \Phi] \Psi_2 \end{aligned} \quad (34)$$

In the presence of the direct contact, these equations become:

$$\begin{aligned} 2m_1\lambda_1(dt)^{(2/D_F)-1} \partial_t \Psi_1 &= [-2m_1\lambda_1^2(dt)^{(4/D_F)-2} \partial^{1l} \partial_{1l} + \Phi] \Psi_1 + \Gamma_{12} \Psi_2 \\ 2m_2\lambda_2(dt)^{(2/D_F)-1} \partial_t \Psi_2 &= [-2m_2\lambda_2^2(dt)^{(4/D_F)-2} \partial^{2l} \partial_{2l} - \Phi] \Psi_2 + \Gamma_{21} \Psi_1 \end{aligned} \quad (35)$$

where  $\Gamma_{12}$  and  $\Gamma_{21}$  are the coupling coefficients of the “bodies.”

Since  $\Psi_1$  and  $\Psi_2$  have a direct physical significations only through as  $|\Psi_1|^2$  and  $|\Psi_2|^2$  probability densities, the deterministic trajectories are replaced by a collection of “potential routes.” In its turn, the concept of “definite position” is replaced by that of probability density. Moreover, the complex fluid particles may be reduced to and identified with their own trajectories (i.e., their geodesics) so that complex fluid should behave as a special “fluid” free of interactions—a fractal fluid. In such a conjecture, quantum-type effects (tunneling effect, entanglement effect, etc.) can be extended to the macroscopic complex fluid.

## 5. Geodesics in the hydrodynamic-type representation

If  $\Psi = \sqrt{\rho}e^{iS}$ , with  $\sqrt{\rho}$  the amplitude and  $S$  the phase of  $\Psi$ , the complex velocity (24) takes the forms:

$$\begin{aligned} \hat{V}_D^i &= 2i\lambda(dt)^{(2/D_F)-1}\partial^i S \\ \hat{V}_F^i &= 2i\lambda(dt)^{(2/D_F)-1}\partial^i \ln \rho \end{aligned} \quad (36)$$

Substituting Eq. (36) into Eq. (21) in the presence of an external potential and separating the real and imaginary parts, up to an arbitrary factor, set to zero by a suitable choice of  $\Psi$  phase, we obtain:

$$\partial_t V_D^i + (V_D^l \partial_l) \hat{V}_D^i = -\partial^l (Q + U) \quad (37)$$

$$\partial_t \rho + \partial^i (\rho \hat{V}_D^i) = 0 \quad (38)$$

with  $Q$ , the specific nondifferentiable potential:

$$Q = -2\lambda^2(dt)^{(4/D_F)-2} \frac{\partial^l \partial_l \sqrt{\rho}}{\sqrt{\rho}} = \frac{V_F^l V_{Fl}}{2} + \lambda(dt)^{(2/D_F)-1} \partial_i V_F^i \quad (39)$$

Eq. (37) represents the specific momentum conservation law, while Eq. (38) represents the states density conservation law. Eqs. (37)–(39) define the fractal hydrodynamic model and imply the following:

- i. any individual component is in permanent interaction with the surrounding fractal medium;
- ii. the fractal medium can be identified with a nondifferentiable fluid, described by Eqs. (37)–(39);
- iii. even if the fractal velocity  $\hat{V}_F^i$  does not reflect a real motion, it influence the specific momentum and energy transfer (confirmed by the its absence from the conservation law of states density); and
- iv. most part of the energy is the form of kinetic and potential energy, other parts in other forms, but the overall energy is constant; the energy and the specific momentum conservation is the one that ensures reversibility and the presence of eigenstates, but does not confirm a Levy type motion in an external field.

## 6. Fractal behaviors

Since, in our model, the fractality plays an essential role in the dynamics of the “complex fluid,” next we will expand the model, admitting the following equations:

$$(V_F^i - \lambda(dt)^{(2/D_F)-1}\partial^i) \partial_l V_F^i = 0 \quad (40)$$

$$\partial_l V_F^l = 0 \quad (41)$$

The first equation presents the fact that “the fractal force” is null, while the second one presents the property of incompressibility of the fractal fluid.

### 6.1. Fractal laminar flow

To find the solutions for these equations can be a relatively difficult, due to the fact that this equation system is a nonlinear one [18–20]. However, there is an analytical solution of this system, in the particular case of a stationary flow in a plane symmetry  $(x, y)$ . In these circumstances, Eqs. (40) and (41), with  $V_F^i = V^i$ , take the form:

$$V_x \frac{\partial V_x}{\partial x} + V_y \frac{\partial V_x}{\partial y} = \lambda(dt)^{(2/D_F)-1} \frac{\partial^2 V_x}{\partial y^2} \quad (42)$$

$$\frac{\partial V_x}{\partial x} + \frac{\partial V_y}{\partial y} = 0 \quad (43)$$

where  $V_x = V_x(x, y)$  is the velocity along axis  $Ox$ ,  $V_y = V_y(x, y)$  is the velocity along axis  $Oy$ . The boundary conditions of the flow are:

$$\lim_{y \rightarrow 0} V_y(x, y) = 0, \quad \lim_{y \rightarrow 0} \frac{\partial V_x}{\partial y} = 0, \quad \lim_{y \rightarrow \infty} V_x(x, y) = 0 \quad (44)$$

and the flux momentum per length unit is constant:

$$\Theta = \rho \int_{-\infty}^{+\infty} V_x^2 dy = const. \quad (45)$$

Using the method from [18–20] for resolving Eqs. (42) and (43), with the limit conditions (44) and (45), the following solutions result:

$$V_x = \frac{\left[1.5 \left(\frac{\Theta}{6\rho}\right)^{2/3}\right]}{[\lambda(dt)^{(2/D_F)-1}x]^{1/3}} \cdot \operatorname{sech}^2 \frac{\left[(0.5y) \left(\frac{\Theta}{6\rho}\right)^{1/3}\right]}{[\lambda(dt)^{(2/D_F)-1}x]^{2/3}} \quad (46)$$

$$V_y = \frac{\left[4.5 \left(\frac{\Theta}{6\rho}\right)^{2/3}\right]}{[3\lambda(dt)^{(2/D_F)-1}x]^{1/3}} \cdot \left[ \frac{\left[y \left(\frac{\Theta}{6\rho}\right)^{1/3}\right]}{[\lambda(dt)^{(2/D_F)-1}x]^{2/3}} \cdot \operatorname{sech}^2 \frac{\left[(0.5y) \left(\frac{\Theta}{6\rho}\right)^{1/3}\right]}{[\lambda(dt)^{(2/D_F)-1}x]^{2/3}} - \tanh \frac{\left[(0.5y) \left(\frac{\Theta}{6\rho}\right)^{1/3}\right]}{[\lambda(dt)^{(2/D_F)-1}x]^{2/3}} \right] \quad (47)$$

Relations (46) and (47) suggest that the fractal fluid velocity field is highly nonlinear by means of soliton and soliton-kink-type solutions. Given the structural complexity of the fluid (given by its various structural units, that retains their own velocity field), an accurate way of writing relations (46) and (47) will be the one in which we assign indexes for each component.

For  $y = 0$ , we obtain in relation (46) the critical velocity of the flow in the form:

$$V_x(x, y = 0) = V_c = \frac{\left[1.5 \left(\frac{\Theta}{6\rho}\right)^{2/3}\right]}{[\lambda(dt)^{(2/D_F)-1}x]^{1/3}} \quad (48)$$

while relation (45), taking into account Eq. (48), becomes:

$$\Theta = \rho \int_{-\infty}^{+\infty} V_x^2(x, y) dy = \int_{-d_c}^{+d_c} V_c^2(x, 0) dy \quad (49)$$

so that the critical cross section of the strain line tube is given by:

$$d_c(x, y = 0) = \frac{\Theta}{2\rho V_c^2} = 2.42 \left[ [\lambda(dt)^{(2/D_F)-1}x]^{2/3} \right] \left(\frac{\rho}{\Theta}\right)^{1/3} \quad (50)$$

Relations (46) and (47) can be strongly simplified if we introduce the normalized quantities:

$$\xi = \frac{x}{x_0}, \quad \eta = \frac{y}{y_0}, \quad u = \frac{V_x}{w_0}, \quad v = \frac{V_y}{w_0}, \quad \Omega = \frac{\left(\frac{\Theta}{6\rho}\right)^{2/3}}{w_0[\lambda(dt)^{(2/D_F)-1}x_0]^{1/3}}, \quad \omega = \frac{\left(\frac{\Theta}{6\rho}\right)^{1/3} y_0}{[\lambda(dt)^{(2/D_F)-1}x_0]^{2/3}} \quad (51)$$

where  $x_0, y_0, w_0$  are the specific lengths and the specific velocity, respectively, of the laminar flow of the fractal fluid. It results that

$$u(\xi, \eta) = \frac{1.5\Omega}{\xi^{1/3}} \sec h^2\left(\frac{0.5\Omega\omega\eta}{\xi^{2/3}}\right) \quad (52)$$

$$v(\xi, \eta) = \frac{4.5^{2/3}}{3^{1/3}} \frac{\Omega}{\xi^{1/3}} \left[ \frac{\omega\eta}{\xi^{2/3}} \sec h^2\left(\frac{0.5\Omega\omega\eta}{\xi^{2/3}}\right) - \tanh\left(\frac{0.5\Omega\omega\eta}{\xi^{2/3}}\right) \right] \quad (53)$$

We present in **Figures 1(a, b)–4(a, b)** the dependence of the normalized velocity field  $u$  on the normalized spatial coordinates  $\xi, \eta$  for various nonlinearity degrees ( $\omega = 0.1, 0.2, 0.5, 5$ ). The results show that the velocity field on the flow direction ( $\xi$ ) is affected in a weak manner by the nonlinearity degree (the velocity always decreases on the flow axes regardless of the nonlinearity degree). On the other hand, the flow direction ( $\eta$ ) is strongly affected. The flow starts from constant values on the  $\eta$  axis, and with the increase of  $\omega$ , preferential flow direction can be identified.

**Figures 5(a, b)–8(a, b)** represent the dependence of the normalized velocity field  $v$  on the normalized spatial coordinates  $\xi, \eta$  for various nonlinearity degrees ( $\omega = 0.1, 0.2, 0.5, 5$ ). For small nonlinearity degrees, the variations (increase/decrease) of the velocity field have similar behaviors on both directions ( $\xi, \eta$ ), while for higher values of the nonlinearity degree, these variations are only focused on a single direction ( $\xi$ ).

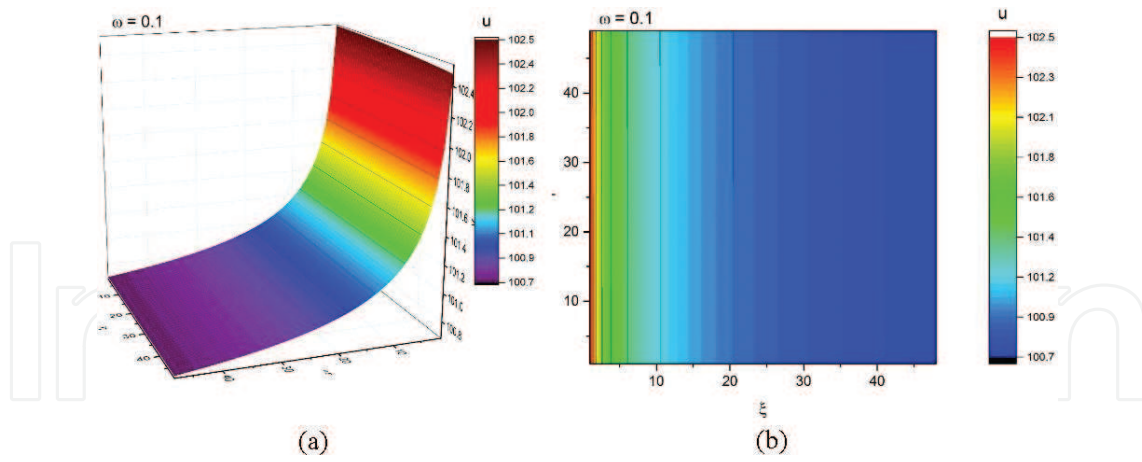


**Figure 1.** The dependence of the normalized velocity field  $u$  on the normalized spatial coordinates  $\xi, \eta$  for the nonlinearity degree  $\omega = 0.1$ : 3D representation (a), the contour plot (b).

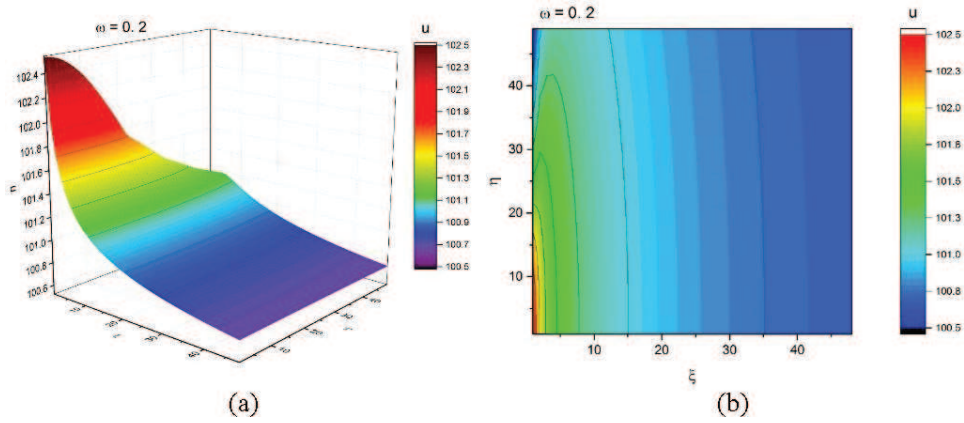


**Figure 2.** The dependence of the normalized velocity field  $u$  on the normalized spatial coordinates  $\xi, \eta$  for the nonlinearity degree  $\omega = 0.2$ : 3D representation (a), the contour plot (b).

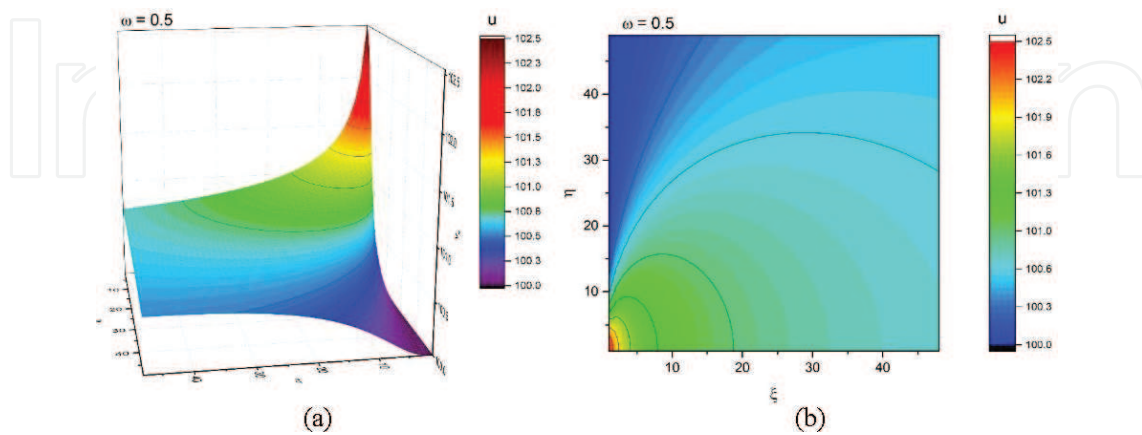


**Figure 3.** The dependence of the normalized velocity field  $u$  on the normalized spatial coordinates  $\xi, \eta$  for the nonlinearity degree  $\omega = 0.5$ : 3D representation (a), the contour plot (b).

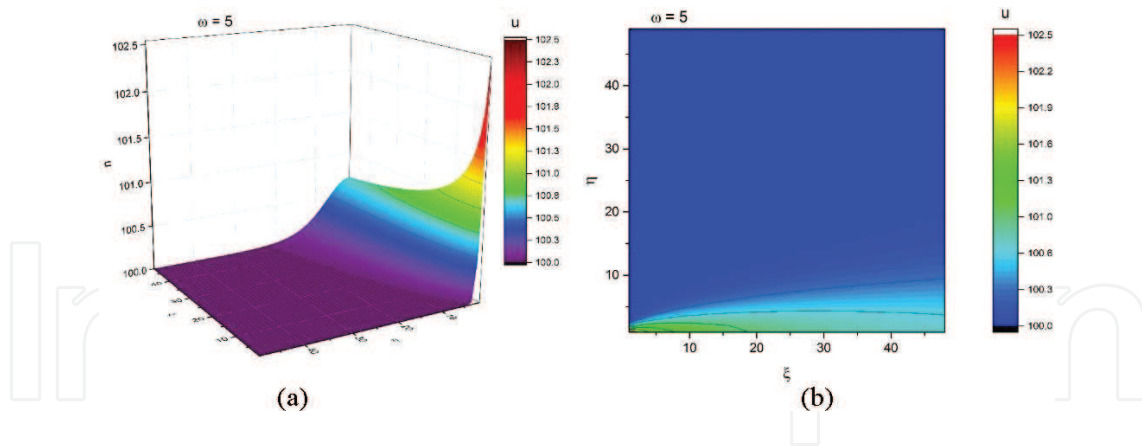


**Figure 4.** The dependence of the normalized velocity field  $u$  on the normalized spatial coordinates  $\xi, \eta$  for the nonlinearity degree  $\omega = 5$ : 3D representation (a), the contour plot (b).

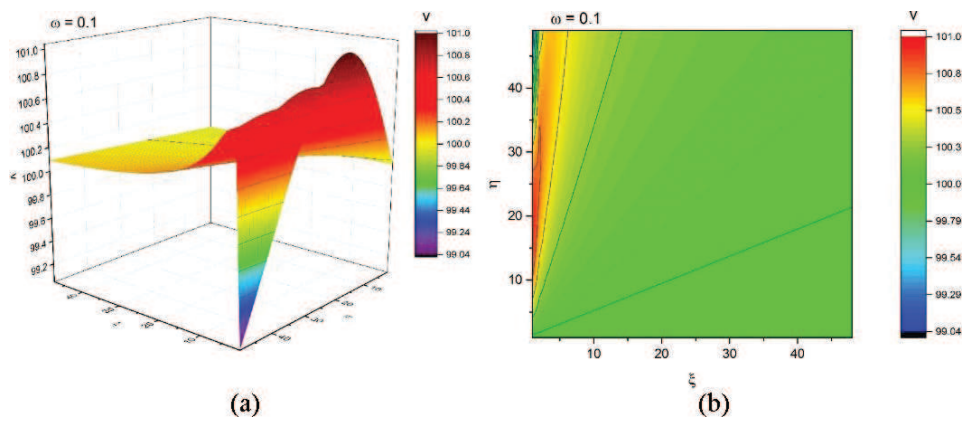


**Figure 5.** The dependence of the normalized velocity field  $v$  on the normalized spatial coordinates  $\xi, \eta$  for the nonlinearity degree  $\omega = 0.1$ : 3D representation (a), the contour plot (b).

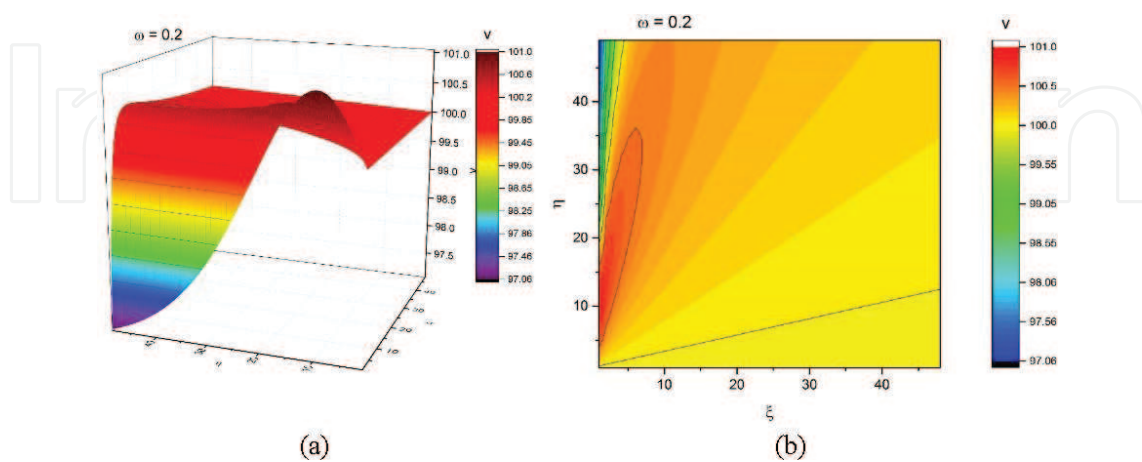


**Figure 6.** The dependence of the normalized velocity field  $v$  on the normalized spatial coordinates  $\xi, \eta$  for the nonlinearity degree  $\omega = 0.2$ : 3D representation (a), the contour plot (b).

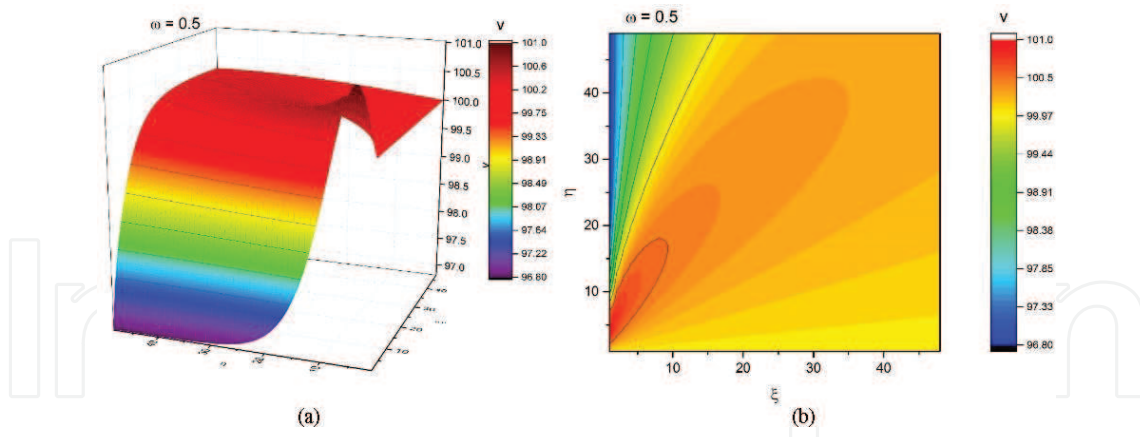


**Figure 7.** The dependence of the normalized velocity field  $v$  on the normalized spatial coordinates  $\xi, \eta$  for the nonlinearity degree  $\omega = 0.5$ : 3D representation (a), the contour plot (b).

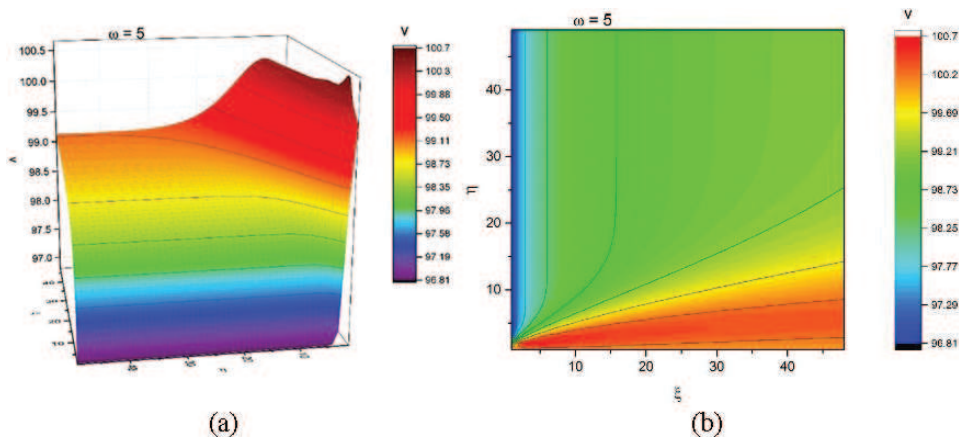


**Figure 8.** The dependence of the normalized velocity field  $v$  on the normalized spatial coordinates  $\xi, \eta$  for the nonlinearity degree  $\omega = 5$ : 3D representation (a), the contour plot (b).

## 6.2. Dynamics of laser ablation plasma assimilated as a fractal fluid

Due to the complexity of the interactions between the particles inside the plume as well as to those between the expanding plume and the background gas, it remains difficult to connect the laser-matter interactions with the plume expansion as well with the interactions between the plume and the laser beam, and the buffer gas. In the case of short laser wavelength, the ablation process can be generally divided in several stages [21]. In the first stages, laser-target interactions, such as laser absorption by the target, target heating, occur. If the laser fluency surpasses the ablation threshold of the target, the laser beam evaporates and ionizes material, generating a plasma plume above the material surface. First, the ejected particles undertake strong collisions in a high-density area near the target creating the Knudsen layer [22]. This leads to a directional evolution, orthogonal to the target surface. After the pulse ends, no more particles are ejected from the target surface. An adiabatic expansion of the plasma happens where the temperatures can be related to the dimensions of the plasma; the thermal energy is

then converted into kinetic energy, with the plasma reaching very high expansion velocities [23, 24]. During the initial stages of plasma expansion, defined by high densities, the mean-free path of the particles is short and the plasma dynamic can be considered as one of a continuum fluid. As the plasma expands, the thermal energy decreases at a quick rate; however, the drop diminishes over time since the energy is recovered in the processes of ions recombination. Once the ambient pressure increases, the plume evolution is determined by the interactions of the laser plasma and ambient gas [25].

Given the complexity of the elementary processes involved in the particle removal and plasma expansion presented above, the dynamic of the laser ablation plasmas can be considered a particular case for the fractal fluid previous presented. An exhaustive model is presented in [26, 27]. In such a conjecture, the evolution of the plasma plume can be seen as series of successive dynamics at various resolutions scales, described by a constant particle density. **Figures 9(a, b)–10(a, b)** present the flow of a fractal fluid at two simultaneously different resolution scales. We observed that the field velocity  $u$  depends on both expansion direction

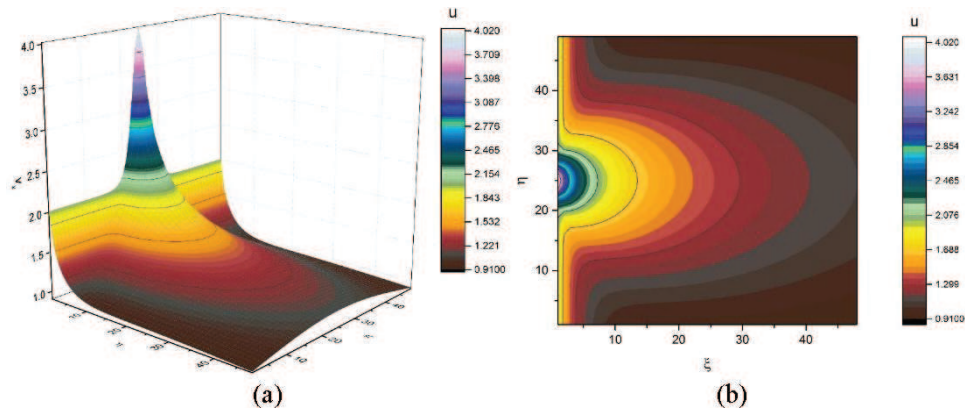


**Figure 9.** The dependence of the normalized velocity field  $u$  on the normalized spatial coordinates  $\xi, \eta$  for two simultaneously resolution scales: 3D representation (a), the contour plot (b).

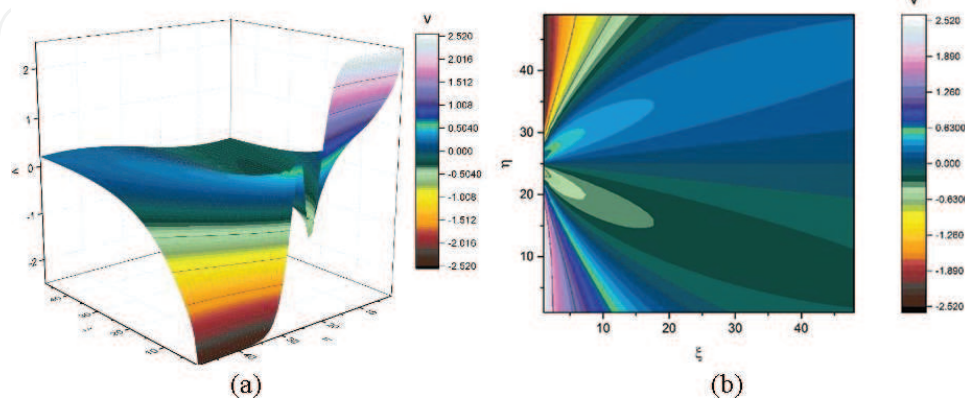


**Figure 10.** The dependence of the normalized velocity field  $v$  on the normalized spatial coordinates  $\xi, \eta$  for two simultaneously resolution scales: 3D representation (a), the contour plot (b).

and its values decrease exponentially. In **Figure 9(a, b)**, it is observed a single maximum, generally attributed to specific plasma structure. The field velocity  $v$  presents a similar evolution on the  $\xi$  axis while on the  $\eta$  direction we observe a split, described by two maxima, attributed to the splitting process often observed for laser-produced plasmas [26, 27].

### 6.3. Blood flow dynamics through fractal fluid approach

Blood is a physical fluid that carries both substances needed by cells for body functioning and, also, metabolic waste products from cells. It consists of 45% blood cells (red and white globules, platelets) and 55% plasma (92% water and various substances in dissipated forms, i.e., protein, glucose, ions, minerals, hormones, carbon dioxide, and cholesterol). Among blood cells, most numerous are red globules containing hemoglobin, a protein with iron in its structure, which facilitates the transport of oxygen by creating ionic bonds with it. In contrast, carbon dioxide is mostly transported extracellular as bicarbonate ion transported in plasma.

Blood is kept in continuous motion in the blood vessels by the heart, through its muscle contraction. Oxygen is transported by the arterial blood to all body cells, from where the waste product, carbon dioxide, is taken by the venous blood and carried to the lungs to be exhaled.

From a physical-chemical point of view, the blood is a suspension, a mixture of liquids, gases, and solids (cells).

In terms of anatomy and histology, blood is considered a specialized form of connective tissue, given its origin in the bones and the presence of potential molecular fibers in the form of fibrinogen.

Since the circulatory system has a fractal structure, it is expected like its functionality to be also fractal. This allows us to assimilate the dynamics of the blood flow with the one of the fractal fluid. In this context, although the velocity fields will remain the same as the one presented in **Figures 1–8**, it is of great importance for the understanding of arterial occlusion and other circulatory system diseases, the force that the fluid will exercise to the walls of the flow vessels.

In our case, the normalized force is given by the relation:

$$F = \partial_{\eta} u - \partial_{\xi} v = - \frac{1.5\Omega \operatorname{sech}^2\left(\frac{0.5\omega\eta}{\xi^{2/3}}\right) \tanh\left(\frac{0.5\omega\eta}{\xi^{2/3}}\right)}{\xi} - \frac{1}{\xi^{1/3}} \left( 0.9\Omega \left( \frac{\frac{\omega\eta \operatorname{sech}^2\left(\frac{0.5\omega\eta}{\xi^{2/3}}\right)}{\xi^{5/3}} + \frac{0.66\omega^2\eta^2 \operatorname{sech}^2\left(\frac{0.5\omega\eta}{\xi^{2/3}}\right) \tanh\left(\frac{0.5\omega\eta}{\xi^{2/3}}\right)}{\xi^{7/3}}}{0.33 \left[ \left(1 - \tanh^2\left(\frac{0.5\omega\eta}{\xi^{2/3}}\right)\right) \omega\eta \right]} \right) 3^3 \right) + \frac{0.3\Omega \left( \frac{\omega\eta \operatorname{sech}^2\left(\frac{0.5\omega\eta}{\xi^{2/3}}\right)}{\xi^{2/3}} - \tanh\left(\frac{0.5\omega\eta}{\xi^{2/3}}\right) \right)}{\xi^{4/3}} \quad (54)$$

In **Figures 11(a, b)–14(a, b)**, it is represented the normalized force field evolution on the two flow direction ( $\xi, \eta$ ) for various nonlinear degrees. It results that with the increase of the

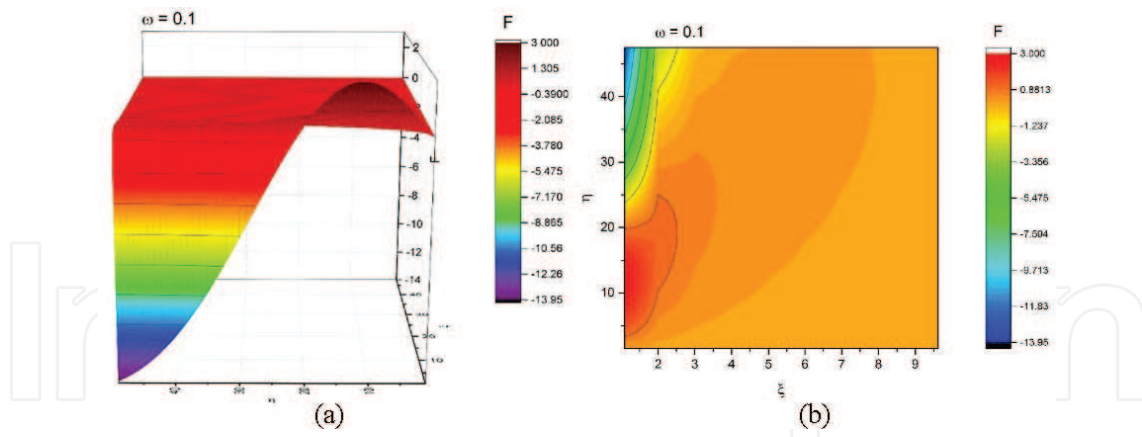


**Figure 11.** The dependence of the normalized force field  $F$  on the normalized spatial coordinates  $\xi, \eta$  for the nonlinearity degree  $\omega = 0.1$ : 3D representation (a), the contour plot (b).

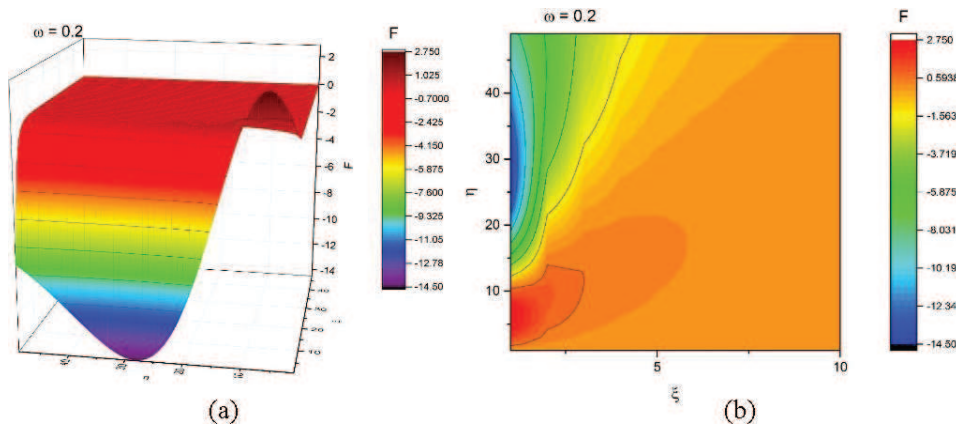


**Figure 12.** The dependence of the normalized force field  $F$  on the normalized spatial coordinates  $\xi, \eta$  for the nonlinearity degree  $\omega = 0.2$ : 3D representation (a), the contour plot (b).

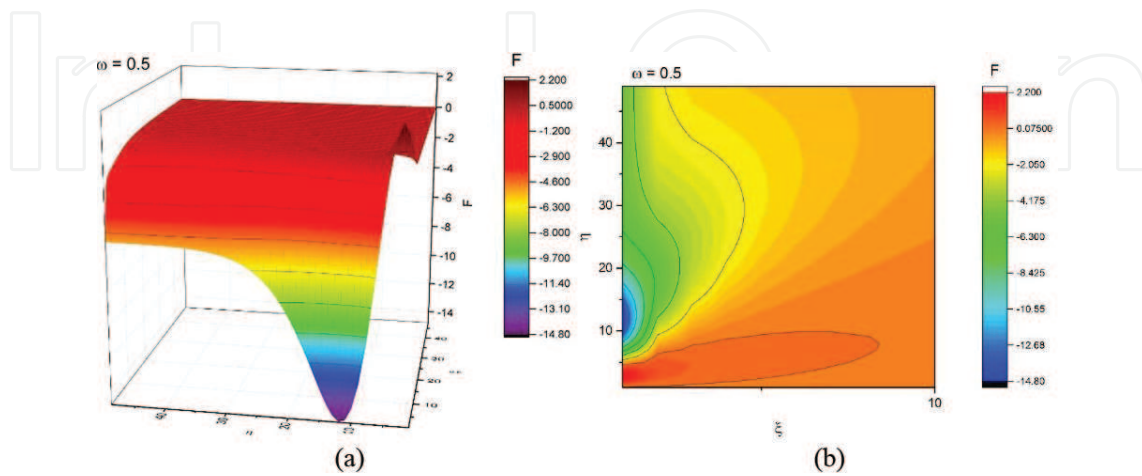


**Figure 13.** The dependence of the normalized force field  $F$  on the normalized spatial coordinates  $\xi, \eta$  for the nonlinearity degree  $\omega = 0.5$ : 3D representation (a), the contour plot (b).

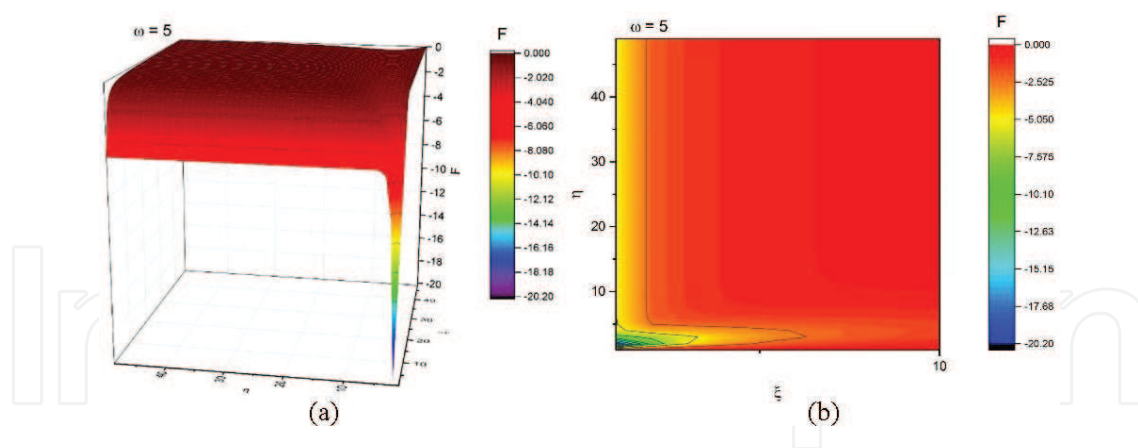


**Figure 14.** The dependence of the normalized force field  $F$  on the normalized spatial coordinates  $\xi, \eta$  for the nonlinearity degree  $\omega = 5$ : 3D representation (a), the contour plot (b).

nonlinearity of the fluid the force toward the walls increases. This can be a starting point for understanding the complexity of the mechanisms involved in the arterial occlusion.

The proposed theory has the advantage that it explains from a fractal point of view the atherogenesis process [28], basically “molding” to the classical anatomical and histopathological descriptions, completely respecting the process postulated by them. Thus, the fractal physics model represents a dynamic and novel argument for sustaining already accumulated morphopathological information and research. The electronic and optical microscopy images (**Figure 15**) describe the spatiotemporal hologram of the phenomenon; we can thus talk about the nonfractal-fractal and microscopic-macroscopic translation through holographically reproducible autosimilarity [28]. We can thus say that fractality represents the mathematical and semantic quintessence for defining atherogenesis, a process that can be physically characterized perfectly by fractal physics, physics becoming in this situation more of a component rather than an explanation for the complex biological system represented by the atheroma plaque [28].

Regarding the recovery of such biological diseases, there are a vast number of techniques. We remind that external electrical stimulation can cause changes in the blood vessels. Although

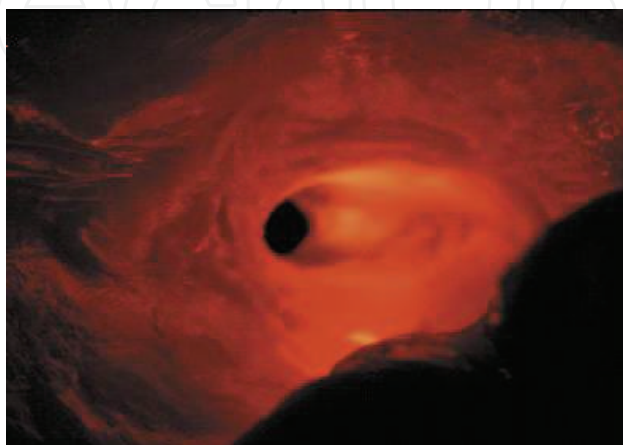


**Figure 15.** Endoluminal view—significant atherosclerotic plaque with thrombus (optical microscopy).

atherosclerosis cause vasodilatation in the affected area and blood flow remains unchanged for an extended period of time, the vascular wall stiffness will increase the pulse pressure [29]. Tracy et al. developed, in 1950, a study whose purpose was to measure the effects of electrical stimulation (ES) on blood flow and blood pressure. All subjects received electrical stimulation at intensity sufficient to produce torque equal to 15% of the predetermined maximal voluntary contraction of their right quadriceps femoral muscle. The conclusions were that the increase in blood flow occurred within 5 min after the onset of ES and dropped to resting levels within 1 min after a 10-min period of ES [30].

Kinesiotherapy or kinesitherapy or kinesiatics is the therapeutic treatment of disease by passive and active muscular movements (as by massage and by exercise) [31].

From the physiotherapeutic point of view, the treatment is directed toward improving blood flow and toward decreasing the disparity between the demand for blood and its supply [32].

An effective vascular rehabilitation training program for improving walking efficiency and vascular remodeling in patients with diabetic atherosclerosis suffering from intermittent claudicating could be a supervised treadmill walking exercise combined with Allen-Burger exercises [33].

## 7. Complex system with the self-elimination of dissipation

If the fractalization is achieved by Markov-type stochastic processes, the scale covariant derivative (18) takes the form:

$$\frac{\hat{d}}{dt} = \partial_t + \hat{V}^l \cdot \partial_l \pm i\lambda(dt)^{(2/D_F)-1} \partial^l \partial_l \quad (55)$$

Postulating now the scale covariance principle the states density conservation laws become:

$$\frac{\hat{d}\rho}{dt} = \partial_t \rho + \hat{V}^l \cdot \partial_l \rho \pm i\lambda(dt)^{(2/D_F)-1} \partial^l \partial_l \rho \quad (56)$$

or more, separating the movement on the scale resolution:

$$\partial_t \rho + V^l \partial_l \rho = 0 \quad (57)$$

for the differentiable scale resolution and:

$$-V_F^l \partial_l \rho \pm \lambda(dt)^{(2/D_F)-1} \partial^l \partial_l \rho = 0 \quad (58)$$

for the nondifferentiable scale resolution. From such a perspective, the fractal-nonfractal dynamic transition of the state density can be obtained by summing Eqs. (57) and (58), taking the form:

$$\partial_t \rho + (V_D^l - V_F^l) \cdot \partial_l \rho \pm \lambda(dt)^{(2/D_F)-1} \partial^l \partial_l \rho = 0 \quad (59)$$

From here, by identifying the movements at the two resolution scales  $V_D^l = V_F^l$ , the fractal-type diffusion equations become:

$$\partial_t \rho \pm \lambda(dt)^{(2/D_F)-1} \partial^l \partial_l \rho = 0 \quad (60)$$

Let us now use Eq. (60) to analyze the dynamic of an electron beam accelerated in a strong electric field which impinges onto a neutral medium. As a result of these interactions, ionizations are produced by: (i) the primary electrons (from the fascicle), which are accelerated by an external electrical field,  $-\alpha j$ , where  $\alpha$  is the primary ionization coefficient and  $j$  is the fascicle current density and by (ii) secondary electrons which results from the direct ionization process,  $-\beta j \rho_e$ , with  $-\beta$  the secondary ionization coefficient and  $\rho_e$  the electron density. In this circumstance, we will further focus on the study of the dynamics induced only by the electronic branch through Eq. (60) written in the following form:

$$\partial_t \rho_e + \lambda(dt)^{(2/D_F)-1} \partial^l \partial_l \rho_e = -\alpha j - \beta j \rho_e \quad (61)$$

Since the previous dynamics implies a dimensional symmetry, Eq. (61) by means of substitutions:

$$\tau = \frac{x}{v} - t, \quad M = \frac{\Lambda}{\beta j v^2} \lambda(dt)^{(2/D_F)-1}, \quad 2R = -\frac{\Lambda}{\beta j}, \quad K = \Lambda, \quad \alpha j + \beta j \rho_e = \Lambda q \quad (62)$$

becomes a damped oscillator-type equation:

$$M\ddot{q} + 2R\dot{q} + Kq = 0 \quad (63)$$

Rewritten as:

$$\dot{p} = -2\frac{R}{M}p - \frac{K}{M}q, \quad q = p \quad (64)$$

Eq. (63) induces a two-dimensional manifold of phase space type  $(p, q)$  in which  $p$  would correspond to a momentum-type variable and  $q$  to a "position" type. Then, the parameters  $M$ ,  $R$ , and  $K$  can have the following significance:

- i.  $M$  characterizes the "inertial" type effect through the connection with ionization processes (global ionization described by  $\alpha j + \beta j$  and the local ones described by  $\beta j$ ) as well as in respect with the fractal diffusion  $(\lambda(dt)^{(2/D_F)-1})$ . All these are done with respect to a traveling wave-type movement based on the self-similar dynamic solutions  $(\tau = \frac{x}{v} - t)$ ;
- ii.  $R$  represents the "dissipative" type effects through the connection with the ionization processes, the same as above;
- iii.  $K$  represents the structural type efforts in connection with the ionization processes, consisting, in this case, only from global ionization effects  $\alpha j + \beta j$ .

The second equation from Eq. (64) corresponds to the momentum definition. Eq. (64) is not a Hamiltonian system, because the matrix traces are not null, and, as consequence, the associated matrix is not an involution. The observation becomes more obvious if we write it in matrix form:

$$\begin{pmatrix} \dot{p} \\ \dot{q} \end{pmatrix} = \begin{pmatrix} -2\frac{R}{M} & -\frac{K}{M} \\ 1 & 0 \end{pmatrix} \cdot \begin{pmatrix} p \\ q \end{pmatrix} \quad (65)$$

With  $M, R, K$  constant values, this matrix equation, written in an equivalent form, evidences the position of the energy, i.e., of the Hamiltonian. From Eq. (64) we can write:

$$\frac{1}{2}M(p\dot{q} - q\dot{p}) = \frac{1}{2}(Mp^2 + 2Rpq + Kq^2) \quad (66)$$

which proves that the energy in its quadratic form, i.e., the right-hand side of Eq. (66) is the variation rate of the physical action represented by the elementary area from the phase space. We would like to show here that the energy does not have to satisfy the conservation laws in order to act like a variation rate for the action. Another issue is the form of the conservation law, if it exists. For this, Eq. (66) will be written as a Riccati-type differential equation:

$$\dot{w} + w^2 + 2\mu w + \omega_0^2 = 0, \quad w = \frac{p}{q}, \quad \mu = \frac{R}{M}, \quad \omega_0^2 = \frac{K}{M} \quad (67)$$

The Riccati-type equation (67) represents always a Hamiltonian system that describes a dynamic of harmonic oscillating type:

$$\begin{pmatrix} \dot{p} \\ \dot{q} \end{pmatrix} = \begin{pmatrix} -\frac{R}{M} & -\frac{K}{M} \\ 1 & \frac{R}{M} \end{pmatrix} \cdot \begin{pmatrix} p \\ q \end{pmatrix} \quad (68)$$

This is a general characteristic of the Riccati-type equations and of the Hamiltonian's dynamic [34]. The 1-differential form for the elementary area from the phase space, obtained from Eq. (68), is identical with Eq. (60). Considering that the energy does not conserve anymore, but another, more complicated, dynamics variable is conserved, Eq. (65), by integration becomes [35]:

$$\frac{1}{2}(Mp^2 + 2Rpq + Kq^2) \cdot \exp \left\{ \frac{2R}{\sqrt{MK} - R^2} \arctan \left( \frac{Mp + Rq}{q\sqrt{MK} - R^2} \right) \right\} = const \quad (69)$$

The energy conservation, in the classical meaning, occurs if either  $R$  is null, either the movement in the phase space takes place on a line through origin, with the slope  $R/M$ .

Moreover, by comparison with the case of the thermal radiation, regarding the distribution function of a preestablished ensemble [36]:

$$P(r, w) = \frac{1}{1 + 2rw + w^2} \exp \left[ \frac{2r}{(1 - r^2)^{1/2}} \arctan \frac{w(1 - r^2)^{1/2}}{1 - rw} \right] \quad (70)$$

with  $r$  the correlation coefficient and  $w^2 = \varepsilon_0/u$  the ratio between the quanta of thermal energy and the reference energy  $u$ , relation (69) becomes:

$$\frac{Kq^2}{2} = \frac{const}{1 + 2rw + w^2} \exp \left[ 2 \frac{r}{(1 - r^2)^{1/2}} \arctan \frac{w(1 - r^2)^{1/2}}{1 - rw} \right], \quad w^2 = \frac{Mp^2}{kq^2}, \quad r^2 = \frac{R}{k} \quad (71)$$

From here we can emphasize the statistic character of energy: the potential energy is constructed as a functional of a specific statistical variable, given by the ratio between the kinetic energy and the potential one of a local oscillator.

Through the correlation of all the oscillator-type ensembles, a “quantization” procedure can be established, by using the condition:

$$P(r, 1) = e^{-\frac{\epsilon_0}{kT}} = \frac{1}{2(1 + r)} \exp \left[ 2 \frac{r}{(1 - r^2)^{1/2}} \arctan \left( \frac{1 + r}{1 - r} \right)^{1/2} \right]$$

where  $k$  is the Boltzmann constant and  $T$  the characteristic temperature of the thermal radiation (for details, see [37]). **Figure 16(a, b)** presents the “quantization” procedure through correlation of all statistical ensembles associated with “local oscillators.”

It shows explicitly the connection between the “quanta” and the statistical correlation of the process represented by the thermal radiation. Moreover, it also specifies the expression of the “quanta” in the small correlation limit, i.e., for  $r \rightarrow 0$ , as  $\epsilon_0 \rightarrow kT \ln 2$ .

Thus, in such limit, the quanta and, implicitly, the frequency  $\nu$  (through  $\epsilon_0 = h\nu$ , where  $h$  is the Plank constant) are proportional with the “color” temperature.

Since we are focused on identifying these dissipative forces, we will try and present a physical significance for the Riccati equation (67) and of the associated Hamiltonian (68). For this, we observe that Eq. (63) is the expression of a variation principle:

$$\delta \int_{t_0}^{t_1} L dt = 0 \quad (72)$$

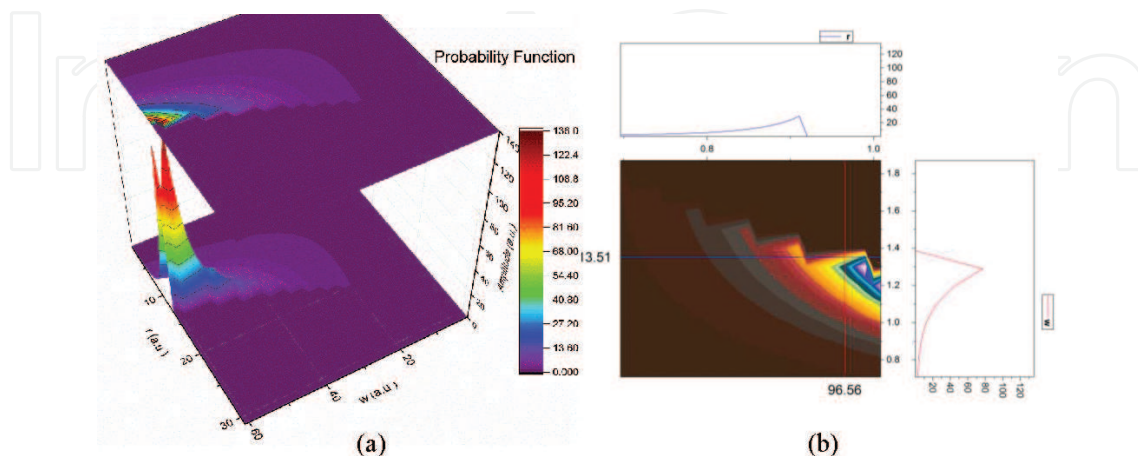


**Figure 16.** The probability function: in  $(r, w)$  space (a), and in the contour plot representation (b).

regarding the Lagrangian:

$$L(q, \dot{q}, t) = \frac{1}{2}(M\dot{q}^2 - Kq^2) \cdot e^{2\frac{R}{M}t} \quad (73)$$

This represents the Lagrangian form of a harmonic oscillator with explicit time-dependent parameters. The Lagrangian integral defined on a finite interval  $[t_0, t_1]$  is the physical action of an oscillator on that specific time interval, describing the difference between the kinetic energy and the potential one. In order to obtain Eq. (63), it is necessary to consider the variation of this action under explicit conditions in such way that the variance of the coordinate at the interval extremes is null:

$$\delta q|_{t_0} = \delta q|_{t_1} = 0 \quad (74)$$

In order to obtain a closed trajectory, a supplementary condition must be imposed; for example, that the coordinates values at the interval extremes are identical:

$$q(t_0) = q(t_1) \quad (75)$$

Moreover, if this trajectory is closed in the phase space, the same condition results also for velocities.

Let us focus now on the movement principle. The Lagrangian is defined until an additive function which needs to be derivative in respect with the time of another function. The procedure is largely used in theoretical physics by defining the gauge transformation. In our case we define a gauge transformation in which the Lagrangian is a perfect square. This is known and explored in the control theory [34]. The procedure consists in adding to the Lagrangian the following term:

$$\frac{1}{2} \frac{d}{dt} \left( w e^{2\frac{R}{M}t} \cdot q^2 \right) \quad (76)$$

where  $w$  is a continuous function in time, so that the Lagrangian is a perfect square. The function variation is null, only due to the conditions presented in Eq. (75) and, therefore, the motion equation does not change. The new Lagrangian, written in relevant coordinates, takes the form:

$$L(q, \dot{q}, t) = \frac{1}{2} M \cdot e^{2\frac{R}{M}t} \left( \dot{q} + \frac{w}{M} q \right)^2 \quad (77)$$

with the condition that  $w$  satisfies the following Riccati-type equation:

$$\dot{w} - \frac{1}{M} w^2 + 2 \frac{R}{M} w - K = 0 \quad (78)$$

The Lagrangian from Eq. (77) can be considered here as representing the whole system energy. As before, there is a relationship between the Riccati equation (78) and the Hamiltonian dynamic. Henceforth, we will find a similar relation to the one presented in Eq. (68):

$$\begin{pmatrix} \dot{\eta} \\ \dot{\xi} \end{pmatrix} = \begin{pmatrix} -\frac{R}{M} & -\frac{K}{M} \\ 1 & \frac{R}{M} \end{pmatrix} \cdot \begin{pmatrix} \eta \\ \xi \end{pmatrix}, \quad w = \frac{\eta}{\xi} \quad (79)$$

In this case, our system is obviously a Hamiltonian one. Thus, we can identify the  $w$  factors with the phase space coordinates. Eq. (78) specifies the fact that  $w$  is a dissipation factor (a mass variation rate, for the variable mass case). It is important to find the most general solution of this equation. Carena and Ramos presented a modern approach to integrate a Riccati equation [38]. Applied to our case, it is enough to note the complex numbers as:

$$w_0 \equiv R + iM\Omega, \quad w_0^* \equiv R - iM\Omega, \quad \Omega^2 = \frac{K}{M} - \left(\frac{R}{M}\right)^2 \quad (80)$$

The roots of the quadratic polynomial from the right-hand part of Eq. (78) are two constant solution of the equation. Being constant, their derivative is null; thus, the polynomial is also null. In order to avoid this situation, we first perform the homographic transformation:

$$z = \frac{w - w_0}{w - w_0^*} \quad (81)$$

In these circumstances, it results that through direct determination,  $z$  is a solution of a linear and homogeneous first-order equation:

$$\dot{z} = 2i\Omega \cdot z : z(t) = z(0)e^{2i\Omega \cdot t} \quad (82)$$

Hence, if we express the initial condition  $z(0)$  in a right manner, we can obtain the general solution of Eq. (78) by applying an inverse transformation to Eq. (81). We find:

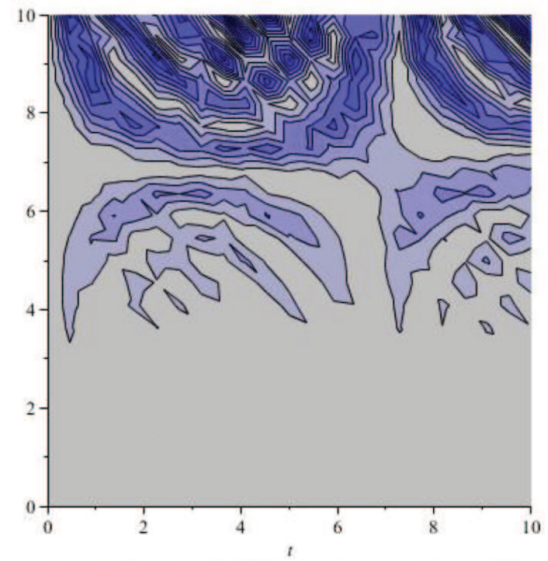
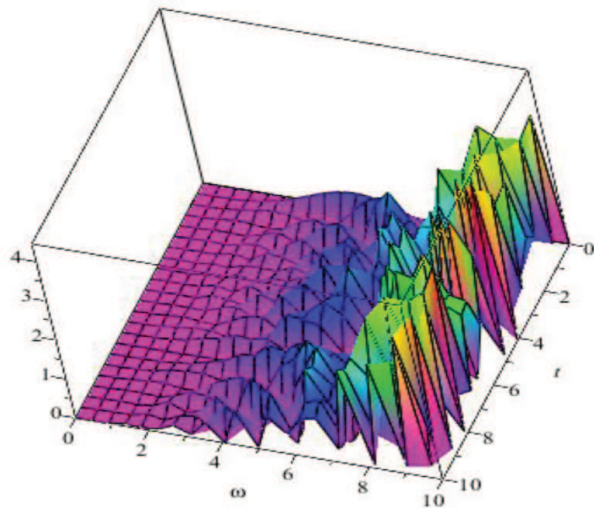
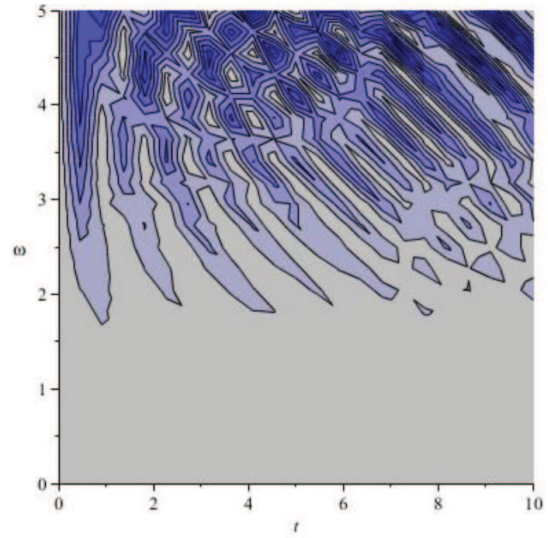
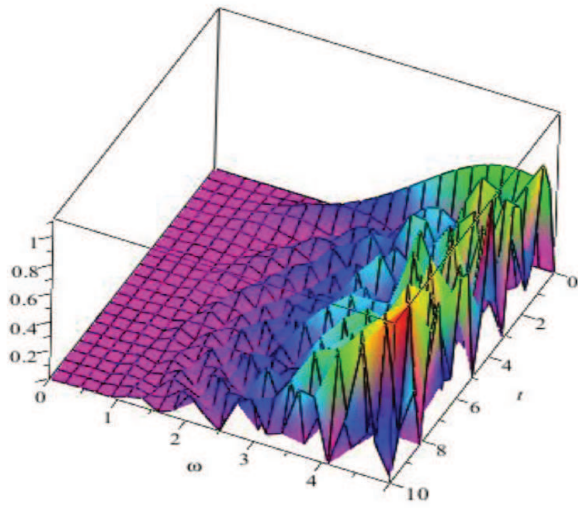
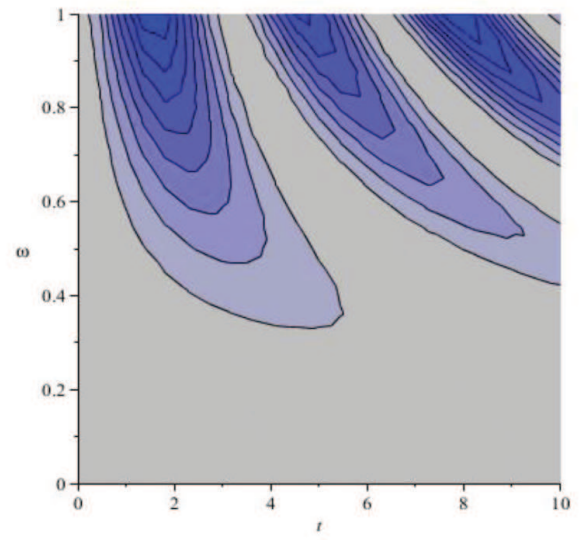
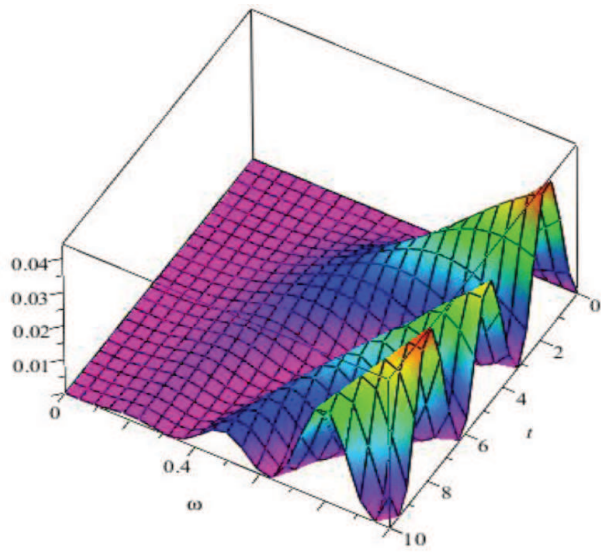
$$w = \frac{w_0 + re^{2i\Omega(t-t_r)}w_0^*}{1 + re^{2i\Omega(t-t_r)}} \quad (83)$$

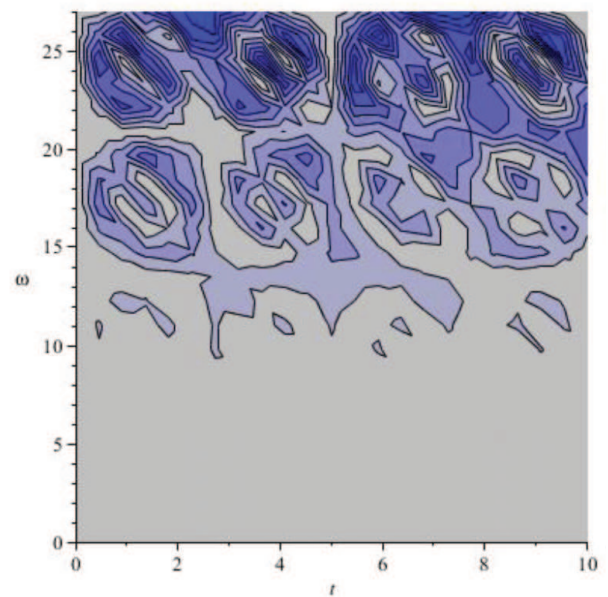
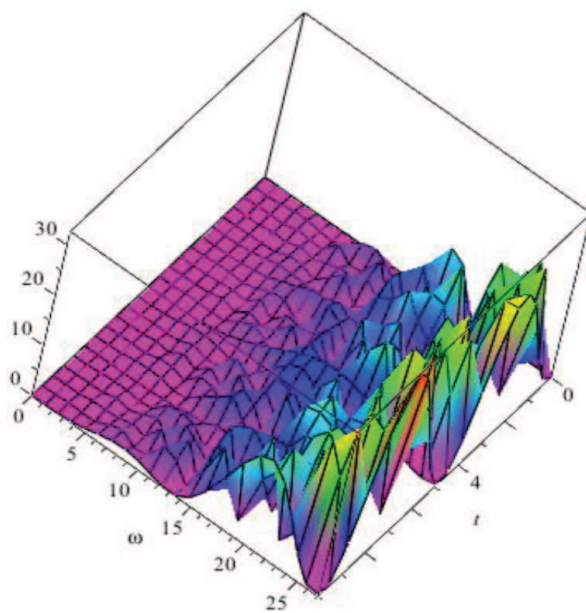
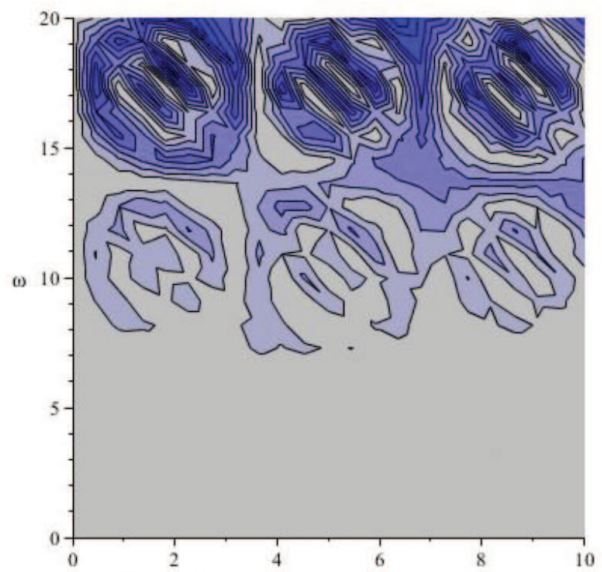
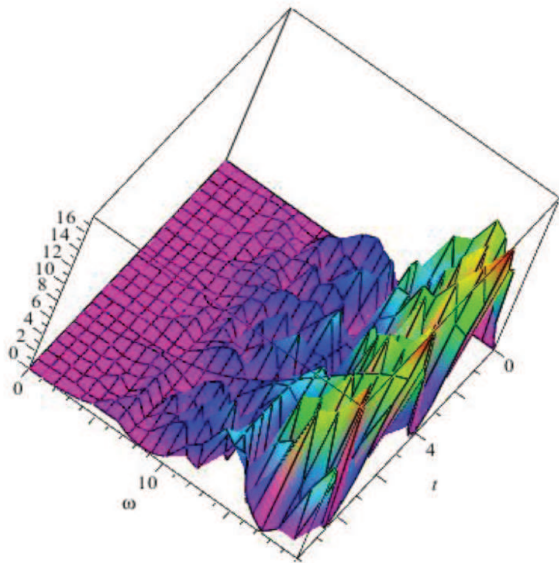
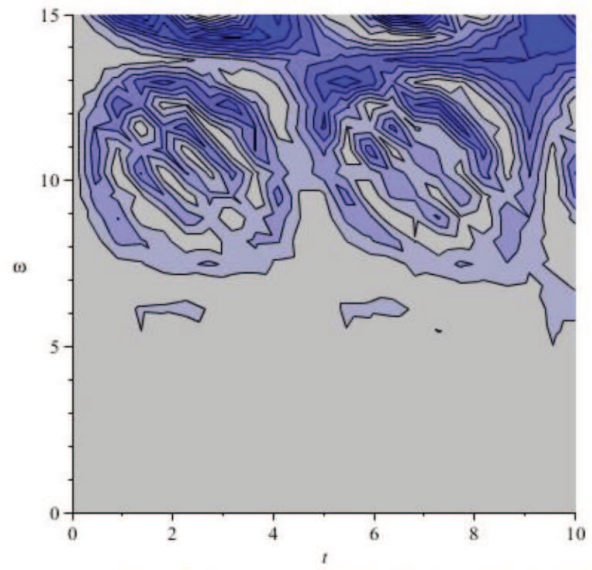
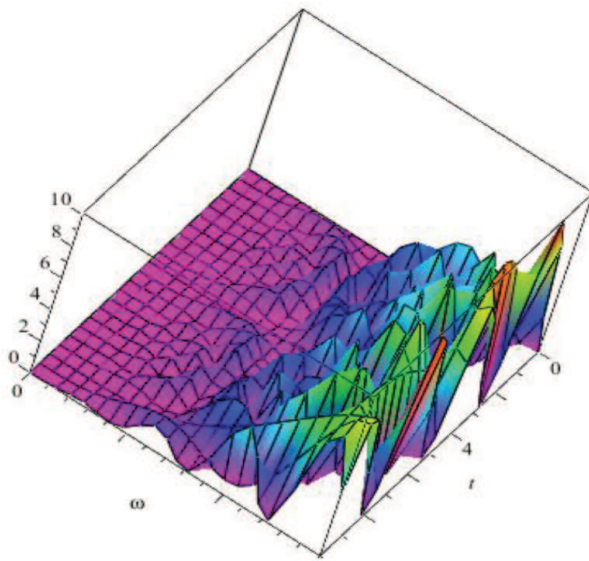
where  $r$  and  $t_r$  are two real constants which are characterizing the solution. Using Eq. (78) we can write the same solution in real terms:

$$z = R + M\Omega \cdot \left( \frac{2r \sin [2\Omega(t - t_r)]}{1 + r^2 + 2r \cos [2\Omega(t - t_r)]} + i \frac{1 - r^2}{1 + r^2 + 2r \cos [2\Omega(t - t_r)]} \right) \quad (84)$$

This relation shows frequency modulation through a Stoler transformation [39], which leads to the complex representation of this parameter.

The theoretical model proposed here analyzes the dynamic of charged particles in a plasma discharge where there is a strong flux of electrons from one plasma structure to another. Basically, the electrons dynamics are described using a forced damped oscillating system, with the aim to investigate the response of the global discharge current to different changes in resolution scale, oscillation frequency and dapping coefficient. Since our mathematical approach is sensitive to the changes in the resolution scales, we plotted in **Figure 17(a-f)** the 3D maps and the





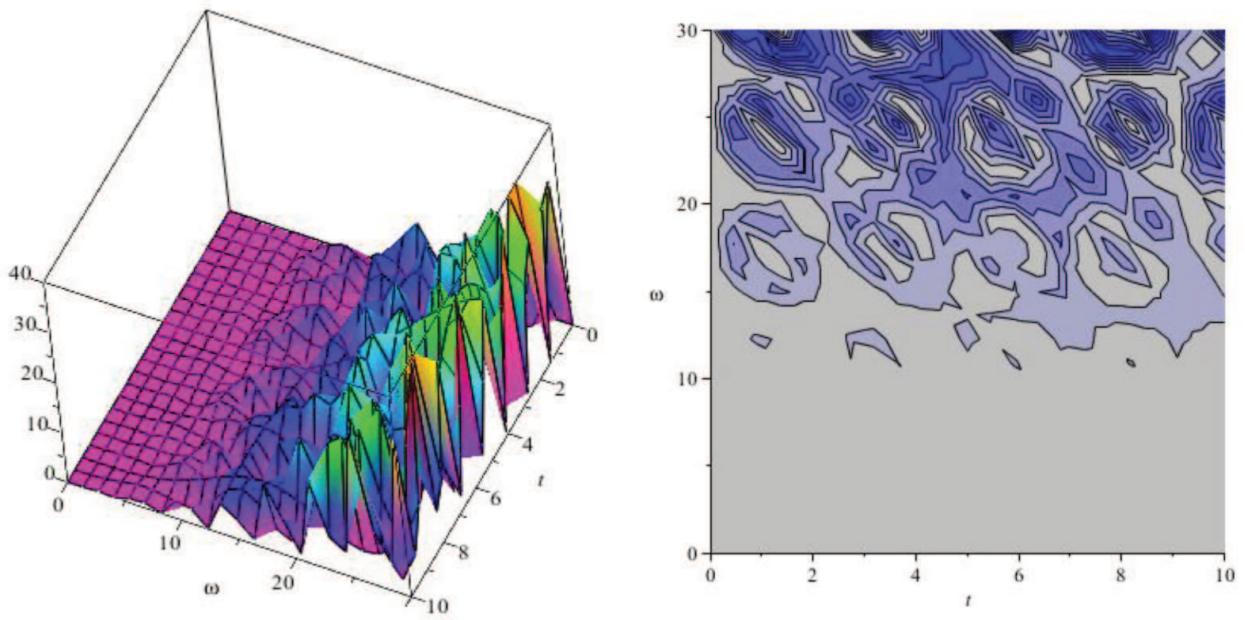


Figure 17. 3D representation of the discharge current for different resolution scales: 0–1 (a), 0–10 (b), 0–15 (c), 0–20 (d), 0–25 (e), 0–30 (f) with respect to the oscillation frequency and the corresponding contour plot representations.

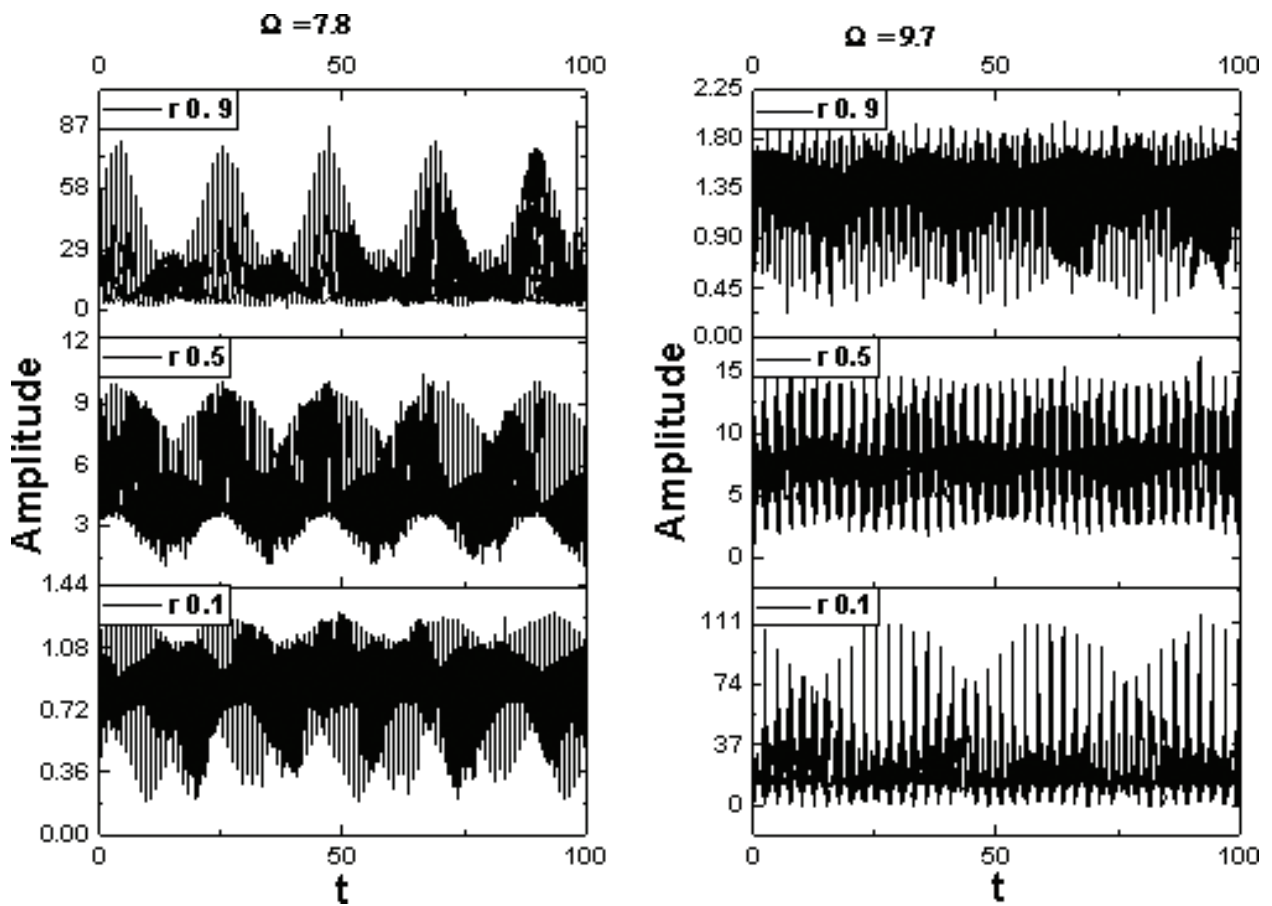


Figure 18. (a and b) Discharge current temporal traces for various values of the damping coefficient extracted for two different frequencies scales.

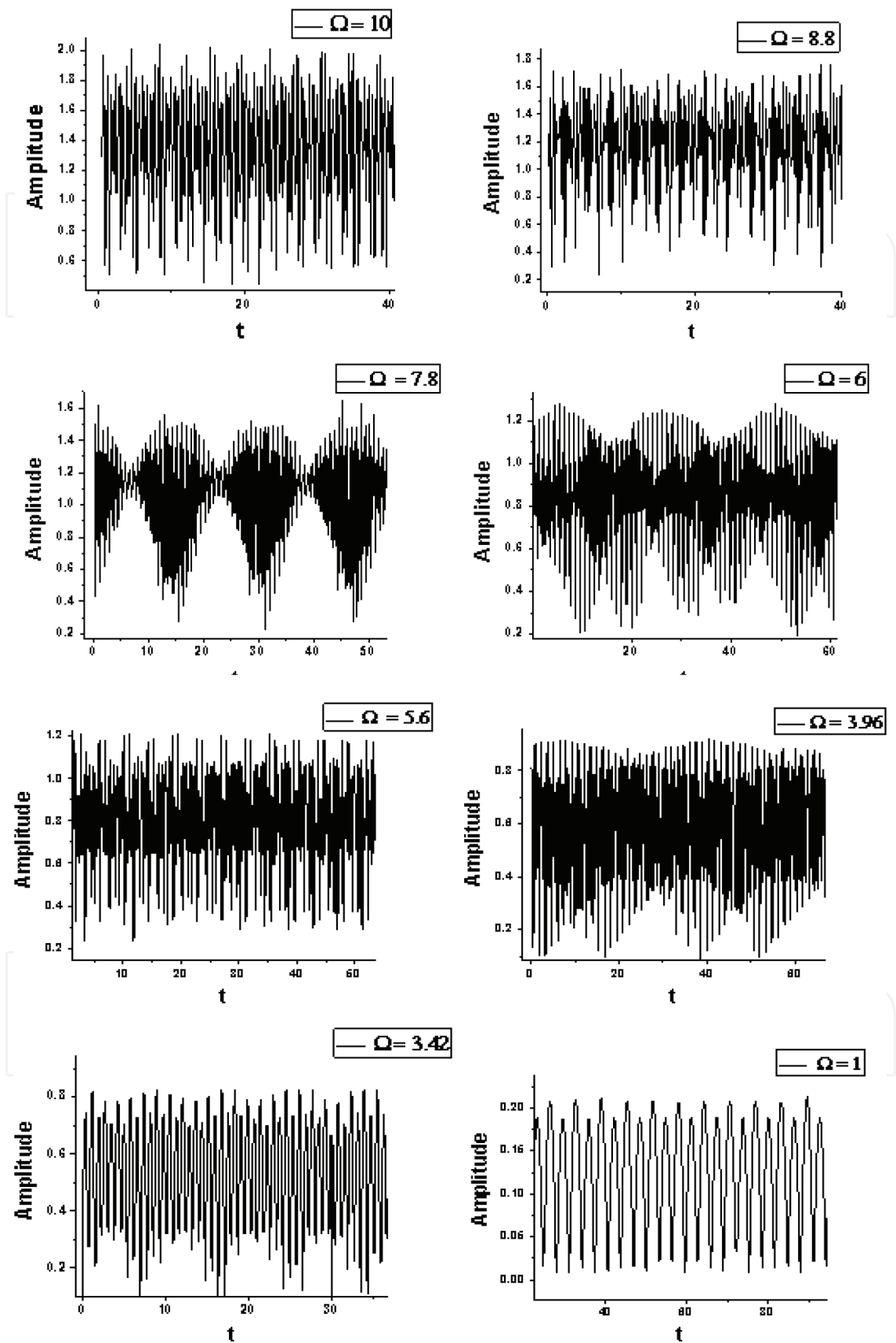


Figure 19. Discharge current temporal traces for different values of the oscillation frequency at a constant damping coefficient ( $r = 0.1$ ).

corresponding contour plot representations of the discharge current as functions of time and oscillation frequency, for a fixed value of the damping constant: 0,1. We observe that, for small resolutions, the current is described by a simple oscillatory regime, and, as the frequency resolution scale increases, we notice the appearance of some patterns. The patterns become denser and are foreshadowing the presence of some modulation in the oscillating frequency.

The damping of the oscillatory state describes the losses through dissipative mechanisms. In order to study the effects induced by these mechanisms on the global current, we pointed two different oscillation frequencies, and observe the temporal response at different values of the damping coefficient. The results can be seen in **Figure 18(a, b)**.

We can identify competing oscillatory behaviors, described by two oscillation frequencies with comparable amplitudes. As the damping increases, the ratio between the two changes oscillation frequencies, and in the end the system oscillates on a single frequency.

The effect of the forced oscillations, which can be attributed to one of the plasma structures, is presented in **Figure 19**, where the discharge current for a fixed value of the damping coefficient and various values of the forced oscillations is represented. The systems seemingly start from a state described by period doubling, and goes through frequency modulation as the values increase. The important aspect is that the oscillation frequencies found for the current are not the ones induced through forced oscillatory system. This means that the system although forced to get on a specific state, it will define its own dynamic influenced, but not determined, by the external parameters.

Finally, we investigated the evolution of our system with the increase of the control parameter  $\omega$ . We investigate for a large range of values the evolution of the system and we observe (**Figure 20a**) that the system starts from double period state (see **Figure 19**), which arises periodically as the values of the control parameter increases. Also, the amplitude of such oscillations increases of about 10 times. In **Figure 20(b)**, the bifurcation map is presented, where we observe that our system starts from steady state (double period state) and passes toward a chaotic one ( $\omega = 7, 22, 44$ ), but never reaches it.

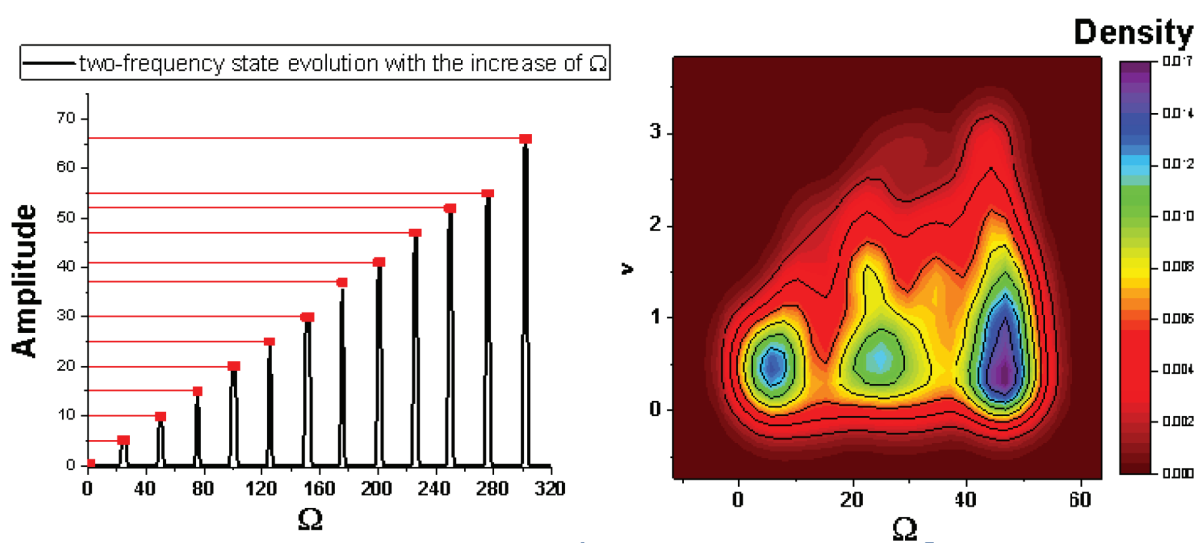


**Figure 20.** The evolution of the double-period state (a) and the characteristic bifurcation map (b) with relation to the control parameter  $\omega$ .

Thus, the evolution of complex system, in our case a plasma, not only intends to reach a chaotic state, but each transition back to the steady state leads to an increase in the system energy, which can be seen in the increase of the amplitude.

## 8. Conclusions

This chapter proposes a new approach for the analysis of dynamics in complex systems based on fractal models, based on the assumption that the “individual components” motion takes place on continuous, but nondifferentiable curves. Consequently, the standard and the “exotic” properties of complex system flow at meso and nano scale can be highlighted.

In this framework, we analyze possible implications of complex fluids in blood flow dynamics. We can affirm that the fractal physics can explain the initiation phase of arteriosclerosis, overcoming the common expression found in classical medicine, “at a certain moment,” which lacks a precise temporal-spatial definition. Moreover, our model imposes redefinition of “good” and “bad” cholesterol, traditionally associated with HDL, respectively LDL. Instead, they should be replaced by the following notions: specific cholesterol entities, associated with a certain nondifferentiable curve, that have a major endothelial impact, i.e., HDL, and specific cholesterol particles which have no or low endothelial impact, i.e., LDL.

We consider that our complex system flow model could also be used for the further development of the study of other complex systems dynamics, such as pulmonary and metabolic diseases or environmental systems.

The evolution of a complex system (plasma discharge or biological systems) was discussed as nonconservative and presented in a simpler way (i.e., through a forced damped oscillating system). Here, the driving force is used to simulate the response of the immune system, while the damping covers the energy losses during the evolution of the tumor cells. Once such a system is chosen, by simply investigating its dynamics, we were able to observe that the systems start from a steady (oscillating state), and as the external factor is varied, the system undergoes significant changes. The system evolves asymptotically through various transition, toward a chaotic regime (like bifurcations or intermittencies), but never reaching it. Another important reveal from the study of the system’s dynamics, was the presence of various steady states depending on the resolution scale at which the theoretical investigations are performed.

Our study not only shows the chaotic evolution tendencies of the complex system, but also reveals that there is a high probability for the presence of steady states. These states arise during the system’s evolution toward chaos, and could be related to dormant stages of the disease and the transitions toward chaos correspond to the uncontrollable growth. The fact that the system would still reach a healthy (steady) state followed by a chaotic evolution couple with an increase in energy would connect to some rebound of cancer in some cases.

## Author details

Maricel Agop<sup>1,2\*</sup>, Decebal Vasincu<sup>3</sup>, Daniel Timofte<sup>4</sup>, Elena Simona Bacaita<sup>1</sup>, Andrei Agop<sup>5</sup> and Stefan Andrei Irimiciuc<sup>6</sup>

\*Address all correspondence to: [m.agop@yahoo.com](mailto:m.agop@yahoo.com)

1 Department of Physics, "Gheorghe Asachi" Technical University of Iasi, Romania

2 Academy of Romanian Scientist, Bucuresti, Romania

3 Department of Biophysics, "Grigore T. Popa" University of Medicine and Pharmacy, Iasi, Romania

4 Department of Surgery, "Grigore T. Popa" University of Medicine and Pharmacy, Iasi, Romania

5 Faculty of Engineering and Material Science, "Gheorghe Asachi" Technical University of Iasi, Romania

6 Faculty of Physics, "Alexandru Ioan Cuza" University of Iasi, Iasi, Romania

## References

- [1] Mitchell M. Complexity: A Guided Tour, Oxford University Press, New York; 2009.
- [2] Thomas Y. H. Multi-scale Phenomena in Complex Fluids: Modeling, Analysis and Numerical Simulations, World Scientific Publishing Company, Singapore; 2009.
- [3] Michel O. D., Thomas B. G. Mathematical Modeling for Complex Fluids and Flows, Springer, New York; 2012.
- [4] Badii R., Politi A. Complexity: Hierarchical Structure and Scaline in Physics, Cambridge University Press, Cambridge; 1997.
- [5] Mandelbrot B. B. The Fractal Geometry of Nature (Updated and augm. ed.). W. H. Freeman, New York; 1983.
- [6] Winfree A.T. The Geometry of Biological Time, 2nd edition, Springer New York; 2000.
- [7] Weibel P., Ord G., Rosler O. E. Space Time Physics and Fractility, Springer, New York; 2005.
- [8] El Naschie M. S., Rossler O. E. Prigogine I., Quantum Mechanics, Diffusion and Chaotic Fractals, Elsevier, Oxford; 1995.

- [9] Cristescu C. P. Non-Linear Dynamics and Chaos. Theoretical Fundamentals and Applications (in Romanian), Romanian Academy Publishing House, Bucharest; 2008.
- [10] Federer J., Aharoner A. Fractals in Physics, North Holland, Amsterdam; 1990.
- [11] Nottale L. Scale Relativity and Fractal Space-Time. A New Approach to Unifying Relativity and Quantum Mechanics, Imperial College Press, London; 2011.
- [12] Nottale L. Fractal Space-Time and Microphysics: Towards a Theory of Scale Relativity, World Scientific, Singapore; 1993.
- [13] Merches I., Agop M. Differentiability and Fractality in Dynamics of Physical Systems, World Scientific, Singapore; 2016.
- [14] Nottale L. Fractals and the quantum theory of space-time. International Journal of Modern Physics A. 1989; **4**: 5047–5117. DOI: 10.1142/S0217751X89002156
- [15] Cresson J. Non-differentiable deformations of  $\mathbb{R}^n$ . International Journal of Geometrical Methods in Modern Physics. 2006; **3**: 1395–1415. DOI: 10.1142/S0219887806001752
- [16] Stauffer D., Stanley H. E. From Newton to Mandelbrot: A Primer in Theoretical Physics with Fractals for the Personal Computer, 2nd edition, Springer, New York; 1995.
- [17] Gouyet J. F. Physique et Structures Fractales, Masson, Paris; 1992.
- [18] Solovastu L. G., Ghizdovat V., Nedeff V., Lazar G., Eva L., Ochiuz L., Agop M., Popa R. F. Non-linear effects at differentiable-non-differentiable scale transition in complex fluids. Journal of Computational Theoretical Nanoscience. 2016; **13**: 1–6. DOI: 10.1166/jctn.2016.4099
- [19] Batchelor G. K. An Introduction to Fluid Dynamics, Cambridge University Press, Cambridge; 2000.
- [20] Landau L.D., Lifshitz E.M. Fluid Mechanics, 2nd edition, Butterworth Heinemann, Oxford; 1987.
- [21] Miller J. C. Laser Ablation. Principle and Applications, Springer-Verlag, Berlin Heidelberg; 1994.
- [22] Anisimov S. I., Bauerle D., Luk'yanchuk B. S. Gas dynamics and film profiles in pulsed-laser deposition of materials. Physical Review B. 1993; **48**: 12076. DOI: 10.1103/PhysRevB.48.12076
- [23] Miotello A., Kelly R. On the origin of the different velocity peaks of particles sputtered from surfaces by laser pulses or charged-particle beams. Applied Surface Science. 1999; **138–139**: 44–51.
- [24] Anisimov S. I., Luk'yanchuk B. S., Luches A. An analytical model for three-dimensional laser plume expansion into vacuum in hydrodynamic regime. Applied Surface Science. 1996; **96–98**: 24–32. DOI: 10.1016/0169-4332(95)00373-8
- [25] Miloshevsky A., Harilal S. S., Miloshevsky G., Hassanein A. Dynamics of plasma expansion and shockwave formation in femtosecond laser-ablated aluminum plumes in argon

- gas at atmospheric pressures. *Physics of Plasmas*. 2014; **21**: 043111. DOI: 10.1063/1.4873701
- [26] Nica P., Agop M., Gurlui S., Focsa C. Oscillatory Langmuir probe ion current in laser produced plasma expansion. *Europhysics Letters*. 2010; **89**: 6500. DOI: 10.1209/0295-5075/89/65001
- [27] Gurlui S., Agop M., Nica P., Ziskind M., Focsa C. Experimental and theoretical investigations of transitory phenomena in high-fluence laser ablation plasma. *Physical Review E*. 2008; **78**: 026405.
- [28] Tesloianu N. D., Ghizdovat V., Agop M. *Flow Dynamics via Non-Differentiability and Cardiovascular Diseases. A Proposal for an Interdisciplinary Approach between Non-Differentiable Physics and Cardiovascular Morphopathology*, Scholars' Press, Saarbrücken; 2015.
- [29] Singh R. B., Mengi S. A., Xu Y.-J., Arneja A. S., Dhalla N. S. Pathogenesis of atherosclerosis: A multifactorial process. *Experimental & Clinical Cardiology*. 2002; **7**(1): 40–53.
- [30] Tracy J. E., Currier D. P., Threlkeld A. J. Comparison of selected pulse frequencies from two different electrical stimulators on blood flow in healthy subjects. *Physical Therapy*. 1988; **68**: 1526–1532.
- [31] Wedlick L. T. Recent advances in medical electricity. *The Australian Journal of Physiotherapy*. 1955; **1**: 152–157.
- [32] Casely E. Atherosclerosis obliterans. *The Australian Journal of Physiotherapy*. 1958; **4**: 19–22.
- [33] Hassan S., Mehani M. Comparison between two vascular rehabilitation training programs for patients with intermittent claudication as a result of diabetic atherosclerosis. *Bulletin of Faculty of Pharmacy, Cairo University*. 2012; **17**: 7–16.
- [34] Zelkin M. I. *Control Theory and Optimization I. Encyclopaedia of Mathematical Sciences, Vol. 86*, Springer-Verlag, Berlin Heidelberg; 2000.
- [35] Denman H. H. Time-translation invariance for certain dissipative classical systems. *American Journal of Physics*. 1968; **36**: 516–519.
- [36] Planck M. *Plancks Original Papers in Quantum Physics*. Wiley and Sons, New York; 1972.
- [37] Mazilu N., Porumbreanu M. *The Becoming of Quantum Mechanics (in Romanian)*, Limes Publishing, Cluj -Napoca, Bucuresti; 2011.
- [38] Cariñena J. F., Ramos A., Integrability of the Riccati equation from a group-theoretical viewpoint. *International Journal of Modern Physics A*. 1999; **14**: 1935–1951. DOI: 10.1142/S0217751X9900097X
- [39] Stoler D. Equivalence classes of minimum uncertainty packets. *Physical Review D*. 1970; **1**: 3217–3219.

